HELMHOLTZ
ZENTRUM FÜR
INFEKTIONSFORSCHUNG

**UNIVERSITÄT
DES
SAARLANDES**

Immortalization of human alveolar epithelial cells: Towards a cell line expressing functional tight junctions for modelling the air-blood barrier *in vitro*

DISSERTATION

zur Erlangung des Grades

des Doktors der Naturwissenschaften der

Naturwissenschaftlich-Technischen Fakultät III

Chemie, Pharmazie, Bio- und Werkstoffwissenschaften

der Universität des Saarlandes

von

Anna Michele Kühn

Saarbrücken

2016

Tag des Kolloquiums: 11.07.2016

Dekan: Prof. Dr.-Ing. Dirk Bähre

Berichterstatter: Prof. Dr. Claus-Michael Lehr

        Prof. Dr. Dr. Robert Bals

Vorsitz: Prof. Dr. Marc Schneider

Akademischer Mitarbeiter: Dr. Jessica Hoppstädter

„Hiermit versichere ich, Anna Michele Kühn, an Eides statt, dass ich diese Arbeit ‚Immortalization of human alveolar epithelial cells: Towards a cell line expressing functional tight junctions for modelling the air-blood barrier *in vitro*' selbstständig und nur unter Angabe der angegebenen Quellen und Verweise angefertigt habe. Die aus anderen Quellen oder indirekt übernommenen Daten und Konzepte sind unter Angabe der Quellen gekennzeichnet. Ich habe diese Arbeit bisher weder im In- noch im Ausland in gleicher oder ähnlicher Form in einem Verfahren zur Erlangung eines akademischen Grades vorgelegt."

Medellín, Mai 2016

Anna Michele Kühn

Die vorliegende Arbeit entstand auf Anregung und unter Anleitung von

Herrn Prof. Dr. Claus-Michael Lehr

am Lehrstuhl für

Biopharmazie und Pharmazeutische Technologie

der Universität des Saarlandes

und am

Helmholtz-Institut

für Pharmazeutische Forschung Saarland

"The presence of those seeking the truth
is infinitely to be preferred to the presence of those
who think they've found it."

-Terry Pratchett, *Monstrous Regiment*

Für Josecito

Table of Contents

Short Summary

This work aims to meet the demand for cell lines reflecting the specific barrier properties of alveolar epithelial cells required for the safety assessment of inhaled drugs, chemicals and (nano-)materials and for investigating biological aspects of the respiratory tract, such as infection pathways in the context of aerosol transmitted infectious diseases.

Given the lack of a suitable *in vitro* model of the air-blood barrier of the peripheral lung that is not comprised of primary cells, a new human alveolar epithelial cell line (hAELVi) with type I-like properties and functional tight junctions was generated using a novel immortalization regimen based on lentiviral transfection of primary alveolar epithelial cells.

hAELVi cells have an unlimited lifespan and maintain the capacity to form tight intercellular junctions, with high transepithelial electrical resistance (> 1000 Ω*cm^2). Ultrastructural analysis and real time PCR revealed type I-like cell properties. Low permeability of the paracellular compound sodium fluorescein confirmed the suitability of hAELVi cells for studying transport of xenobiotics across the air-blood barrier *in vitro*.

These results suggest that hAELVi cells reflect the essential features of the air-blood barrier, as crucial for e.g. epithelial transport studies, and hence may become a valuable tool in the field of pulmonary research.

KURZZUSAMMENFASSUNG

Diese Arbeit zielt darauf ab, die Nachfrage nach Zelllinien, die die spezifischen Barriereeigenschaften von Alveolarepithelzellen aufweisen, zu bedienen, die für die Sicherheitsbewertung von inhalativen Medikamenten, Chemikalien und (Nano-) Materialien, und für die Untersuchung biologischer Aspekte der Atemwege, wie z.B. Infektionsmechanismen, erforderlich sind.

Da ein *in vitro*-Modell der Luft-Blut-Schranke (LBS) der peripheren Lunge mit Barriereeigenschaften bisher nur durch Primärzellen erzeugt werden konnte, wurde eine immortale humane Alveolarepithelzelllinie (hAELVi) mit Typ-I-ähnlichen Eigenschaften und funktionellen Tight Junctions erzeugt, mittels lentiviraler Transfektion unter Verwendung einer neuartigen Immortalisierungstrategie. hAELVi-Zellen haben eine unbegrenzte Lebensdauer, bilden interzelluläre Verbindungen, und folglich einen hohen transepithelialen Elektronenwiderstand ($> 1000\ \Omega^* cm^2$). Ultrastrukturelle Analysen und halb-quantitative realtime-PCR belegen Typ I-ähnliche Zelleigenschaften. Die geringe parazelluläre Permeabilität von Natriumfluorescein bestätigt die Eignung der hAELVi-Zellen für *in-vitro* Untersuchungen des Transports von Xenobiotika über die LBS.

Die hier präsentierten Ergebnisse legen nahe, dass hAELVi-Zellen Merkmale der LBS wiederspiegeln, was als entscheidend für z.B. Transportstudien über die Epithelzellschicht anzusehen ist, und somit ein nützliches neues Instrument auf dem Gebiet der Lungenforschung darstellen könnten.

I. INTRODUCTION

I.1 The lung and the respiratory epithelium

I.1.1 Structure and function of the lungs

The purpose of the lungs is the respiratory gas exchange that means to provide the red blood cells with oxygen, and to remove carbon dioxide. The organ is comprised of two lungs, called the lobes. Air enters the boy through the nose or the mouth by inhalation. After entering the nose or mouth, air travels down the trachea, which divides into the right and left bronchus. The bronchi branch into smaller secondary and tertiary bronchi and those divide dichotomy into bronchioles. In these upper airways no gas exchange takes place, they are mainly a filter system, secreting mucus and removing airborne particulates via the muco-cilliary clearance mechanism. Each of the bronchioles divides into two to eleven alveolar ducts. There are five or six alveolar sacs associated with each alveolar duct. The alveolar epithelium comprised of alveolar type I (ATI) cells and alveolar type II (ATII) cells are the gas exchanging units of the lung. The alveolar epithelium is in direct contact with the endothelium of the lung capillaries and due to its extremely thin walls, the respiratory gases are exchanged via diffusion through these two cell layers driven by concentration gradients. Alveolar macrophages are important immune cells that patrol the surface of the alveolar epithelium, motile, phagocytizing foreign matter, like particles and microbial infectious agents (Sato et al., 2002; Hoppstädter et al., 2010; Kannan et al., 2009).

In total the airways reach a length of approximately 2400 km. Normal lungs contain over 300 million alveoli, which together reach a surface area of the air-blood barrier of about 70 m^2. The lung is comprised of 27 different cell types (Jones et al., 1996), of which are some shown in Figure I-1. Furthermore the change of the morphology of the lung along the way from the upper airways to the alveoli is schematically demonstrated in the same figure. A variety of drug transporters in the lung was described (Bosquillon, 2010), highlighting its high potential as site of drug deposition and delivery, either local or systemic (Patton et al., 2004).
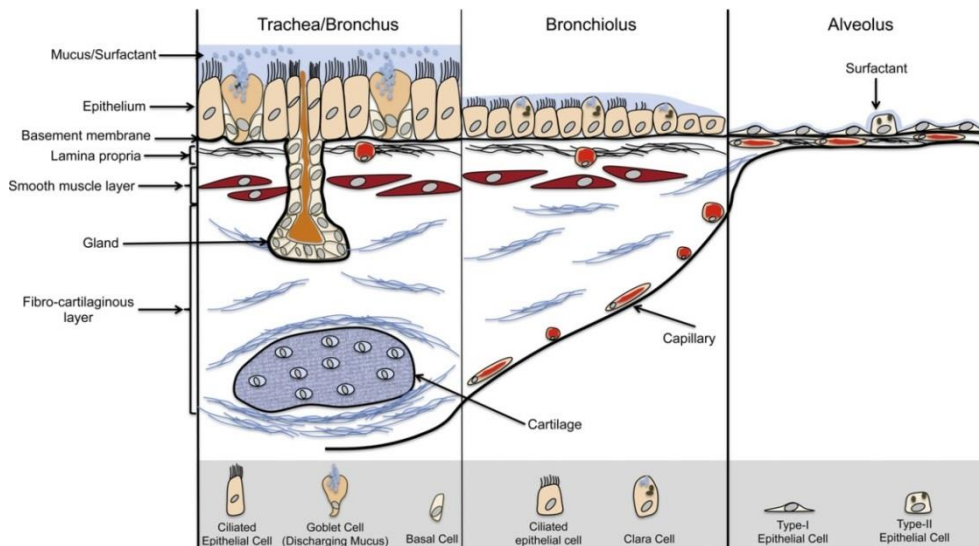
Figure I-1: Structure and different cell types of the lung.
Airway wall structure and main cell types of the lung at three principal levels. The epithelial layer gradually becomes reduced from pseudostratified to cuboidal and then to squamous. The airway epithelium is comprised of epithelial and secretory cells. Cartilage and smooth muscle layer are only present in the upper to lower airways, but not in the alveoli. Adapted from Klein *et al.* (Klein et al., 2011), modified from Ochs and Weibel (Ochs and Weibel, 2008)

I.1.2   Alveolar cells type I and type II

The alveolar epithelium of the peripheral lung is mainly comprised of two cell types, alveolar type I (ATI) and alveolar type II (ATII) cells, both forming the air-blood barrier which is responsible for gas exchange. The more cuboidal ATII have a diameter of approximately 10 to 20 µm covering 6% to 7% of the total alveolar surface area and counting for 16% of all lung cells (Crapo et al., 1982). ATII cells produce lung surfactant proteins to reduce the alveolar surface tension (Phelps and Floros, 1991). ATII cells synthesize the surfactant components and store them in specialized organelles, the so called lamellar bodies. Secretion of the surfactant proteins occurs via membrane fusion after the lamellar bodies are transported to the apical membrane. ATII cells not only produce the surfactant proteins, but subject them to a recycling process of reuptake, intracellular processing and resecretion of the recycled material (Andreeva et al., 2007). Those are the main components, but ATII cells also produce other components of the alveolar lining fluid, like hyaluronic acid (Bray, 2001). ATII cells play a role in the innate and adaptive immunity of the lung, e.g. they activate alveolar macrophages upon infection with *P.aeruginosa*, *M. avium* and *M. tuberculosis* (Kannan et al., 2009; Sato et al., 2002; Kato and Schleimer, 2007). In the case of acute lung injury the ATII cells act as progenitors of ATI cells, in a stem cell-like manner (Barkauskas et al., 2013). This ability is used for the

primary culture of ATI-like cells, where ATII cells are isolated and then differentiated into ATI-like cells (Daum et al., 2012; Elbert et al., 1999). The abovementioned functions of the ATII cells brought them the title "defender of the alveolus" (Fehrenbach, 2001; Mason, 2006). The first isolation and culture protocol was described by Kikkawa and Yoneda in 1974 (Kikkawa and Yoneda, 1974; Dobbs, 1990).

The very large squamous ATI cells (80 to 100 µm diameter (Crapo et al., 1982)) essentially represent the barrier between blood and air space of the lung; those form a tight epithelium. They cover about 92% of the alveolar surface, but counting only for 8% of the total number of lung cells. This is possible due to their very thin (50-100 nm) cytoplasmic extensions (Crapo et al., 1982) ATI cells shield the organism from outer influences by forming a tight barrier sealed up by intercellular connections, so called tight junction complexes (Crandall and Matthay, 2001; Godfrey, 1997). While paracellular transport is thus restricted, transport of solutes mainly occurs via transcellular pathways, either by passive diffusion or by active transport via various transporter proteins (Endter et al., 2009). ATI cells are terminally differentiated (Weibel, 1974), being incapable of either proliferation or cell plasticity. Furthermore ATI cells contribute to the lung homeostasis and regulation of ion transport and water flow, the metabolism of peptides, the modulation of macrophage functions, and intercellular signaling (Dobbs et al., 2010; Williams, 2003).

The culture of ATII and ATI cells is described for different animal species, including rat, pig, hamster, swine and human for ATII cells (Chen et al., 2004; Murphy et al., 1999; Kikkawa and Yoneda, 1974) and rat, mouse, swine and human for ATI cells (Chen et al., 2004; Daum et al., 2012; Elbert et al., 1999; Steimer et al., 2007, 2006; Demaio et al., 2009)

I.2 Lung cell models

Primary cells are often the gold standard of *in vitro* cell models, because their advantage is that they mimic the *in vivo* situation in the best possible way. They reflect the physiological phenotype of the native cell in most of the cases. Therefore, results obtained with primary cell models have the highest significance or informative value in terms of reflecting the *in vivo* situation (Eglen and Reisine, 2011; Goldbard, 2006). However, primary cells also have certain disadvantages that have to be taken into consideration. The reproducibility of results obtained with primary cells could be questionable due to the donors' genetic heterogeneity. The availability of healthy human tissue to isolate the desired cell type is a big problem, as well as the cost and time factor of the isolation procedure itself. The limited lifespan and the limited amount of cell material often impede the use of primary cells in high-throughput screenings and long-term studies (Goldbard, 2006; Eglen and Reisine, 2011).

Cell lines offer the advantage of an unlimited lifespan and proliferation, so that high amounts of cell material can be produced in a short time. The reproducibility of results from cell lines is expected high, because they are homogenous and have constant characteristics.

The following chapters will introduce different cell models of the lung, primary as well as cell lines, their advantages and disadvantages, and their significance as models of the air-blood barrier in the field of pharmaceutical research.

I.2.1   hAEpC - a primary cell model of the alveolar epithelium

The primary cell model of human alveolar epithelium (hAEpC) was first described in 1999 by Elbert (Elbert et al., 1999). Till date it is the most reliable alveolar cell model reflecting the *in vivo* situation of the air-blood barrier (ABB), especially regarding the study of absorption and transport of xenobiotics (Kim et al., 2001; Forbes and Ehrhardt, 2005). Its main advantage is its ability to form a functional barrier, caused by tight junctions, which can be determined by the so called trans-epithelial electrical resistance (TEER), a widely accepted parameter for tightness of an epithelium. Based on the ability of ATII cells to transdifferentiate into ATI cells, e.g. upon injury (Barkauskas et al., 2013; Clegg et al., 2005), ATII cells are isolated from healthy human lung tissue and seeded onto fibronectin/collagen-coated Transwell® filter membranes, where they differentiated into ATI-like cells upon 2 to 10 days in culture. Since then the hAEpC isolation procedure and culture conditions were subsequently refined and improved (Daum et al., 2012). The transition from ATII to ATI-like cells was monitored with cell type-specific lectin binding patterns, the development of TEER and immunostaining of tight junction proteins (Elbert et al., 1999); later the transition was confirmed with analysis of ultrastructure and cell type-specific marker expression (Fuchs et al., 2003). The suitability to use this model for drug delivery applications, e.g. for the transport of high and low permeability markers, proteins and peptides, was also evaluated (Ehrhardt, 2003; Elbert et al., 1999; Bur et al., 2006) and complemented with the expression analysis of ABC, SLC and SLCO drug transporters (Endter et al., 2009). Even in the context of infection research the primary cell model was used. Peiris *et al.* investigated the pro-inflammatory response induced by influenza viruses(Chan et al., 2005).

Since no other alveolar cell model mirrors the properties of the alveolar epithelium in such an extent, the hAEpC cells were deployed in advanced co-culture models for various purposes, e.g. to investigate the interaction of epithelial cells and immune cells, like human blood monocyte-derived macrophages and dendritic cells, in the presence of xenobiotics or inhaled particles (Lehmann et al., 2011; Blank et al., 2011) or to investigate immune- and inflammatory response in co-cultures of hAEpC cells and blood mononuclear cells (Torvinen et al., 2007).

Unfortunately, the isolation procedure of the hAEpC cells is time-consuming and expensive and limited by the availability of healthy human lung tissue from donors undergoing lung resection surgery. Because of the limitation of the cell material, also the experimental design is limited, by the amount of isolated cells and their short lifespan, so that high-throughput screenings or longtime studies are difficult to realize. Inter-individual differences and health status of the donors can negatively affect the reproducibility of results. All those issues cause that, despite the hAEpC model is the gold standard cell model of the alveolar epithelium, the use of cell lines of the lung is often the method of choice. The next chapter deals with different cell lines to model the alveolar epithelium.

I.2.2   Lung cell models based on cell lines

A number of human (Ehrhardt et al., 2003; Forbes, 2003; Foster et al., 1998; Grainger et al., 2006) and non-human (Rosenberger et al., 2014; Horálková et al., 2009) lung epithelial cell lines are commercially available; however, in terms of mimicking the tight barrier formed by ATI cells they are of limited function. R3/1 is a rat alveolar cell line incapable of developing high TEER values, as they are observed in cultured primary cells of rat lung but used in studies of migrating immune cells (Horálková et al., 2009; Lührmann et al., 2007). LET1 is a murine cell line of epithelial type I cells, obtained via lentiviral transfection with SV40 LTAg, used to study innate immune response to influence ,but is not yet characterized regarding its barrier properties (Rosenberger et al., 2014) The human alveolar cell line A549, derived from an adenocarcinoma and commonly used in toxicity studies (Roggen et al., 2006), does not exhibit high TEER values and is therefore not well suited for drug absorption studies (Foster et al., 1998). A549 cells have a rather ATII-like phenotype, including such important type II features, like lamellar bodies (Shapiro et al., 1978) However, they have been used in drug transport studies (Forbes and Ehrhardt, 2005; Kobayashi et al., 1995; Wang and Zhang, 2004; Kim et al., 2001), particle interaction and toxicity assays (Moschini et al., 2013; Wemhöner et al., 2011), and respiratory infections (van den Bogaard et al., 2009; Kemp et al., 2008) despite the fact of its amiss barrier formation. Table I-1 lists some examples of the most commonly used cell models of the human lung.

Other widely used lung cell lines are 16HBE14o- and Calu-3, but they are of bronchial origin (see Figure I-1), and therefore - although they build TEER of 300-600 $\Omega * cm^2$ – they are not suitable as a model of the alveolar epithelium (Forbes, 2003; Ehrhardt et al., 2003; Grainger et al., 2006). However, they are also commonly used for drug absorption and transport studies (Pohl et al., 2009; Chowdhurya et al., 2010; Florea et al., 2003)

A new human ATI cell line (TT1), recently described by Tetley *et al.* (van den Bogaard et al., 2009), has been obtained through the immortalization of primary ATII cells and used as a model for inflammatory response studies and nanoparticle uptake (Kemp et al., 2008). However, TT1 cells do not appear to develop tight intercellular junctions, and therefore still lack important barrier properties (van den Bogaard et al., 2009; Kemp et al., 2008).

Table I-1: Different human cell models of the peripheral lung

cell model	origin	cell type/ morphology	TEER	Suitable model for the ABB?
hAEpC	human lung tissue isolation	ATII cells developing into ATI-like cells	high (> 1500 $\Omega\cdot cm^2$) (Elbert et al., 1999)	yes
16HBE14o-	human bronchial epithelium, SV40 LTAg	bronchial epithelium	intermediate (~ 500 $\Omega\cdot cm^2$) (Ehrhardt, 2003)	limited
Calu-3	human adenocarcinoma	bronchial epithelium, secretory	intermediate (400 – 1000 $\Omega\cdot cm^2$) (Grainger et al. 2006; Ehrhardt et al. 2002)	limited
A549	human adenocarcinoma	ATII (lamellar bodies, no biochemical properties of ATII)	No (Foster et al., 1998)	limited
H441	human papillary adenocarcinoma	Clara Cells/ATII cells, secretory	low (~ 150 $\Omega\cdot cm^2$) (Neuhaus et al., 2012)	limited
TT1	human ATII cells, $T_{sens.}$ SV40 LTAg and hTert	ATI-like, inflammatory response	low (~ 50 $\Omega\cdot cm^2$) (van den Bogaard et al., 2009)	limited

Another human papillary adenocarcinoma line, H441, with ATI-like phenotype, but lacking functional barrier properties, is widely used in advanced co-culture systems, mainly to study particle interaction and immune response (Papritz et al., 2010; Neuhaus et al., 2012; Kasper et al., 2011; Hermanns et al., 2004). In the following chapter some of these advanced co-culture models and their significance for the pharmaceutical research will be introduced.

I.2.3 The significance of models of the air-blood barrier for the pharmaceutical research

Cell models of the human airways and peripheral lung are of utmost importance for the pharmaceutical research. The use of human cell models, including primary cells, cell lines in monoculture and advanced co-culture models, can lead to a reduction of *in vivo* animal models (Cryan et al., 2007) and avoid the problem of species' incompatibilities. Today, mostly co-culture models are used to study drug absorption and transport in the lung (Daum et al., 2009; Ehrhardt et al., 2002; Lehmann et al., 2011), toxicity of airborne particulate matter and inhaled (nano-)materials (Lehmann et al., 2011; Blank et al., 2011; Brandenberger et al., 2010; Kasper et al., 2011; Klein et al., 2011; Papritz et al., 2010; Rothen-Rutishauser et al., 2008), as well as inflammation and infection (Hittinger et al., 2015; Hermanns et al., 2004, 2009; Chan et al., 2005). Drug delivery systems to cure lung diseases or to enable systemic delivery of pharmaceuticals via the respiratory route (Patton et al., 2004; Patton and Byron, 2007) depend on reliable *in vitro* test systems mimicking the air-blood barrier or the interaction of epithelial and immune cells of the lung, and on devices to applicate drug formulations or to model aerosol or particulate matter inhalation (Bur et al., 2009; Hein et al., 2011), important for toxicity or infection studies. One major requirement all those cell models and culture systems have to comply with is the barrier integrity of the alveolar epithelium. It is pivotal to generate a human alveolar cell line, since till date there is no one available that achieves the desired barrier properties, to implement it in advanced co-culture models to improve all the above mentioned aspects of pharmaceutical research.

I.3 Immortalization

Despite all the advantages primary cell cultures offer in terms of physiological relevance, their limited life span is a major disadvantage. Cell lines with immortal life span are easier to cultivate, because time- and cost-intensive isolation procedures are not necessary, and their homogeneity provides higher reproducibility of results. Long-term studies, as well as high-throughput screenings are possible with the implementation of cell lines.

I.3.1 Lentiviral vectors for transfection

Lentiviral vectors are gene delivery vehicles derived from HIV-1 are can be used to infect a wide variety of dividing and non-dividing cells. They can integrate the transgene stably into the host genome, resulting in long-term expression. All dispensable genes were removed from the HIV-1 genome to produce vector particle that are replication deficient and self-inactivating. The lentiviral vector systems of the third generation used nowadays consist of four plasmids (Dull et al., 1998). The transfer vector contains the transgene to be delivered in a lentiviral backbone containing the sequences required for genomic RNA production and packaging. Lentiviral transfer vectors can be designed to express transgenes, constitutively or conditionally, in single units or multiple combinations. The other three plasmids (pMDL containing gag/pol, pRev and pVSVG) provide the factors required for packaging (Tiscornia et al., 2006).

I.3.2 "Classical" immortalization strategies

In order to achieve immortalization, the mechanisms that limit the proliferation potential of a certain cell type must be omitted (Horrocks et al., 2003; Stacey and MacDonald, 2001).For some cell types, such as murine fibroblasts, immortalization can be achieved by continuous passaging of primary cells *in vitro* by the 3T3 protocol (Todaro, 1963). Immortal cell lines can be carcinoma-derived, like the A549 alveolar cell model (Foster et al., 1998), obtained e.g. by spontaneous mutation of tumor suppressors such as p53 (Harvey and Levine, 1991) and pRb (Nevins, 1994) or by overexpression of viral oncogenes (Linder and Marshall, 1990; Horrocks et al., 2003). Classical immortalization strategies involve the transfection with strong oncogenes or combinations of strong oncogenes, like the simian virus 40 Large T-Antigen (SV40 LTAg) or the E6/E7 oncogenes from the human papilloma virus (Jha et al., 1998; Nevins, 1994; Shay et al., 1991; Vass-Marengo et al., 1986). LTAg, unfortunately is alone only useful to immortalize rodent cells and has been proven very inefficient for the immortalization of humane cells; furthermore it causes drastically altered

phenotypes when employed in human cells (Gazdar et al., 2002). Combination of LTAg with other immortalizing genes like human telomerase (hTert), c-myc or E6/E7 showed to be successful in some cases (Kiyono et al., 1998; Gazdar et al., 2002). Unfortunately the transfection with strong oncogenes often leads to dedifferentiation, aberrant cell growth or transformation (altering the cells tumorigenic), which is different from immortalization (Strauss and Griffin, 1990) and thus diminishes the physiological relevance of the cell lines (Stacey and MacDonald, 2001).

I.3.3 "New" immortalization strategies

A recently described alveolar cell line, suitable for inflammation and nanoparticle uptake studies, named TT1, was generated by the combined transfection of ATII cells with hTert and a thermo sensitive mutant of the SV40 LTAg. (Kemp et al., 2008). The resulting phenotype resembles more that of ATI cells, but fails to develop barrier properties of ATI-like cells (van den Bogaard et al., 2009).

Using temperature sensitive mutants of oncogenes is one method to control the immortalization in order to reduce side effects like dedifferentiation. Another method is the conditional immortalization, where the translation is under the control of a doxycycline (also tetracycline, in the following abbreviated with tet)-dependent promoter system. This immortalization strategy bears the advantage that the promoter that is regulating the expression of the transgene can be "switched" on and off, depending on the presence or absence of doxycycline (May et al., 2010). This systems was successfully employed in the completely reversible immortalization of murine fibroblast with the SV40LTAg (May et al., 2004).

Besides using promoter systems that allow conditional expression, also the use of transgenes that are so called "mild proliferators" is a novel approach to accomplish immortalization without drastically changing the cellular phenotype. This method is based on the combination of several transgenes affecting the cell cycle control mechanisms when expressed together, but not alone. Hauser *et al.* were able reproduce the immortalization of a murine intestinal epithelium cell line with a certain set of transgenes (Schwerk et al., 2013).

I.3.4 Immortalization strategy for hAEpC

For the immortalization of primary human alveolar type I cells we implemented four different combinations promoter systems and transgenes. The transgenes were either "classical" oncogenes (SV40LTAg and hTert) or a set of 33 "mild proliferators" that was described previously in the dissertation of Franziska Klein "Eine innovative Strategie zur Etablierung physiologisch relevanter Säugerzelllinien" (Klein, 2012), under either the translational control of a constitutively expressing SV40 promoter or a conditionally tet-dependet promoter. Figure I-2 demonstrates the different approaches of the immortalization strategy. The successful approach consisting of constitutive expression of a set of 33 different "mild proliferators" led to the generation of a new human alveolar type I-like cell line with functional barrier properties.

Immortalization Strategy

Different promoter systems

Constitutively expressed promoter system (SV40 promoter)

Conditionally expressed promoter system (tetracyclin-dependent promoter, either auto- regulated or regulated by a transactivator)

Different transforming genes

Classic transformation genes (hTert, Large T-Antigen)

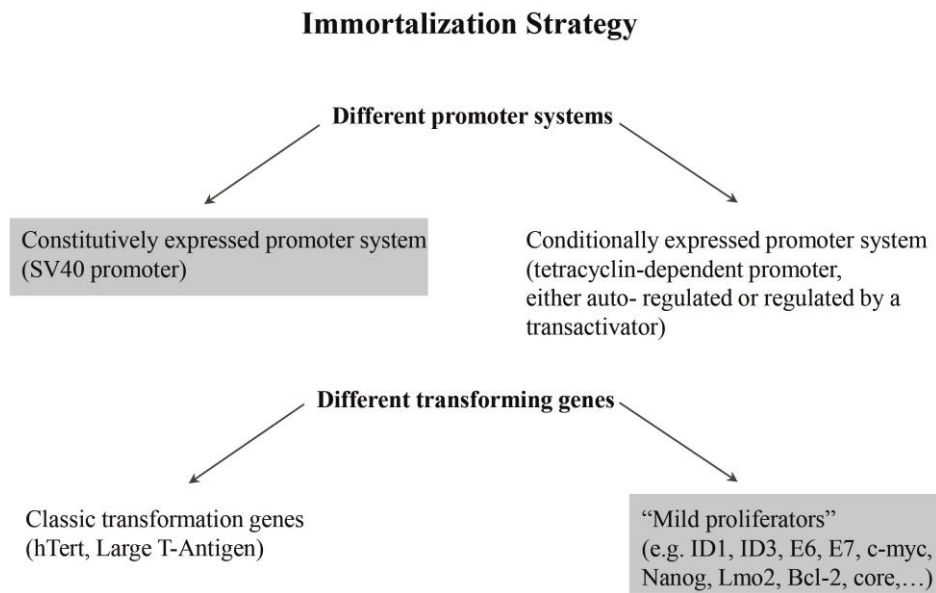"Mild proliferators" (e.g. ID1, ID3, E6, E7, c-myc, Nanog, Lmo2, Bcl-2, core,…)

Figure I-2: Immortalization strategy.
The different immortalization strategies, which were used in this work, are depicted here. The vectors used contained either classic transformation genes or so called "mild proliferators" under the translational control of either a constitutive or a conditional promoter system. Grey boxes indicate the successful strategy.

I.4 Aim of the work

The aim of this work was the establishment and characterization of a new human alveolar type I-like cell line exhibiting a functional barrier due to the expression of tight junction complexes. Till date there was no such cell line available. Classical as well as new immortalization strategies were used to reduce the possibility of de-differentiation and loss of physiological relevance due to phenotypical alterations.

II. Experimental section

II.1 Materials and Methods

II.1.1 Isolation of hAEpC cells:

Primary alveolar epithelial cells (hAEpC) were isolated according to the established protocol by Daum *et al.* (Daum et al., 2012). Tissues were used with ethical approval from the Ärztekammer des Saarlandes and patients' agreement, previously informed about the procedure. Lung tissue material obtained from the healthy parts of resected lung areas of patients undergoing lung tumor resection surgery is washed in a sterile Petri dish containing BSSB (Balanced salt solution buffer: 137 mM NaCl, 5.0 mM KCl, 0.7 mM $Na_2HPO_4 \cdot 7H_2O$, 10 mM HEPES, 5.5 mM glucose, 1.2 mM $MgSO_4 \cdot 7H_2O$, 1.8 mM $CaCl_2 \cdot 2H_2O$, 5 mlPen/Strep (Gibco, Darmstadt, Germany) solution . pH 7.4 at 37°C and filtered through a 0.2 µm filter) for several times to reduce the number of blood cells. Using scissors the tissue is cut in small pieces of approximately 1 cm^3 and then chopped with the McIlwain ® tissue chopper (cut size 5 µm) and collected in BSSB. The minced tissue is rinsed several times in BSSB by subsequent straining through cell strainers and when clean undergoes enzymatic digestion in BSSB/trypsin/elastase solution at 37°C. After 40 minutes the reaction is stopped with inhibition solution (DMEM/F12, FCS, DNase) and homogenized by pipetting with a 25 ml pipette. The suspension is filtered to get rid of remaining tissue and the obtained crude alveolar cell extract is concentrated by centrifugation (5 min at $300 \times g$), suspended in adhesion buffer (DMEM/F12:SAGM 1:1, 2% DNase) and distributed equally to cell culture Petri dishes for adhesion of macrophages at 37°C. After 90 min the supernatant is carefully collected and concentrated by centrifugation (5 min at $300 \times g$). The in BSSB resuspended cell solution is then fractionated using a Percoll® (Sigma) gradient centrifugation (20 min at $300 \times g$). The cells form a slightly visible layer at the interface of the two Percoll® concentrations and are harvested with a Pasteur pipette. To remove the Percoll® remnants the cell solution is washed by centrifugation and resuspension in BSSB. As a final step the epithelial cells in the cell solution are incubated with anti-CD326 conjugated magnetic MicroBeads® (Miltenyi Biotec, Bergisch Gladbach, Germany) and selected with the matching separation column system (MiniMACS Starting Kit, Miltenyi Biotec). The isolated epithelial cells, which are mainly ATII cells are seeded on fibronectin/collagen-coated (Becton Dickinson, Heidelberg, Germany/Sigma) six-well cell culture plates or Transwell® filters (either 1.12 cm^2 (3460) or 0.33 cm^2 (3470), Corning) at a density of $6 \cdot 10^6$ cells/cm^2 and maintained in Small Airway Growth Medium (SAGM, Lonza, Verviers, Belgium),

supplemented with 10% (v/v) fetal calf serum (FCS) and 1% (v/v) penicillin/streptomycin (P/S) in an incubator (5% CO_2, 95% relative humidity, 37°C).

II.1.2 Lentivirus production:

Production of lentiviral vectors was carried out by transient transfection of four helper plasmids and the corresponding expression cassette in HEK293T cells (Human embryonal kidney cell line, ATCC number CRL 11268) as previously described by May *et al.* (May et al., 2007) described. All the plasmids were provided by the working group of Dr. Dagmar Wirth "Model Systems for Infection and Immunity" from the Helmholtz-Centre for Infection Research, Braunschweig, Germany and by Dr. Tobias May, shareholder of InSCREENeX GmbH, Braunschweig, Germany, which commercializes such immortalized cell lines. Tobias May filed a patent for the immortalization of mammalian cells which covers the immortalization regimen (CI-SCREEN gene library; InSCREENeX GmbH; International patent application PCT/EP2011/005528 "Methods and Vectors for Cell Immortalisation").

$5x10^6$ HEK293T cells were seeded onto a 6-well culture plate in DMEM plus 1% (v/v) penicillin/streptomycin and placed in the incubator (5% CO_2, 95% relative humidity, 37°C) for 24 hours. After 24 hours the helper plasmids pLP1 (gag/pol), pLP2 (rev), pLP/VSVg (VSVg) and the plasmid with the appropriate expression cassette were slowly pipetted into a 2.5M $CaCl_2$ solution. Subsequently, this DNA solution was added dropwise under constant vortexing into a HEBS solution (280 mM NaCl, 50 mM HEPES, 1.5 mM Na_2HPO4; pH 7.1). The DNA-HEBS solution was then added on top of HEK293T cells, and then these were coated with fresh medium and cultured overnight. During the following two days the virus-containing supernatant was harvested, filtered and stored at -80°C. Using NIH3T3 cells (Embryonic mouse fibroblast (MEF) cell line, ATCC CRL 1658), the virus titer of the harvested supernatant was then determined and used for the infection of hAEpC cells. Prior to infection master mixes of the lentiviral supernatants produced in HEK293T cells were prepared; in each case the same volume of the virus were added to the mix.

II.1.3 Infection of hAEpC

The hAEpC cells seeded on 6-well cell culture plates were infected on day 5 of culture with the self-inactivating lentiviral vectors, which were previously produced. For infection, the lentiviral supernatant was mixed 1:1 with SAGM culture medium and 8 µg/ml polybrene (Sigma) and added on top of the hAEpC cells. The following day the infection media was aspirated and the cells were further cultivated with the abovementioned culture media for five weeks before colonies of proliferating cells became apparent. These cells were pooled and further cultivated as polyclonal cell lines.

II.1.4 Cultivation of hAELVi cells:

The transfected cells were passaged 1:1 in the first months of culturing when they reached confluence, and afterwards cultivated in a 1:3 ratio every 14 days. Medium was changed every two to three days.

hAELVi cells were cultured on 6-well cell culture plates, T25 cell culture flasks or T75 cell culture flasks for maintaining and propagation and passaged accordingly. For characterization experiments they were cultured on Transwell® filters (either 1.12 cm² (3460) or 0.33 cm² (3470), Corning) or cell culture chamber slides To set up the air-liquid interface (ALI) condition, hAELVi cells seeded on Transwell® filter were exposed to the air on the apical side and fed with SAGM only from basolateral compartment. For the liquid-liquid culture condition (LLC) the cells were totally submerged in culture medium from the apical as well as the basolateral side. The cells were cultivated for 2 days under LLC (with cell culture medium feeding from both, apical and basolateral sides). After that, the cells were divided into two groups: some wells remained under LLC cultivation, while others were transferred to the ALI condition. The cells were cultured in SAGM (Lonza) supplemented with 10% (v/v) fetal calf serum (FCS) and 1% (v/v) penicillin/streptomycin (P/S) in an incubator (5% CO_2, 95% relative humidity, 37°C).

II.1.5 Growth curve:

To obtain the growth curves, hAELVi cells, passage 18 ($1x10^4$ cells per well) were seeded on 24-well plates; thereafter the cells were trypsinized and counted 24h after seeding and then every 48h with the CASY® Cell counter (Roche) (n=3).

II.1.6 Genomic DNA isolation and agarose gel electrophoreses

DNA of hAELVi cells, at passage number 28, was isolated using the DNeasy Blood & Tissue kit (Qiagen Cat.No. 69504) following the manufacturer's protocol. PCR was performed using the Taq PCR Master Mix kit (Qiagen Cat.No. 201445), starting with an initializing denaturation for 4 min at 95°C followed by 35 cycles of denaturation for 30 sec at 95°C, annealing at 65°C for 60 sec, elongation step of 90 sec at 72°C, and finished with a final elongation for 7 min. As template, 1 µg genomic DNA of the immortalized cells was used. For each gene a separate PCR was run. The PCR were analyzed on a 1 % agarose gel and the genes were scored either as absent or present. Primers to identify the integrated transformation genes were ordered from Eurofins; and are listed in Table II–1. Both primers bind in the expression cassette that is introduced by the lentivirus. The 5' primer is located in the SV40 promoter whereas the 3' primer is specific for the respective immortalizing gene.

Table II-1: Primers used to detect the immortalizing genes.

Both primers bind in the expression cassette of the gene. The 5' primer in each case is the same, binding the SV40 promoter. The 3' primer is gene-specific.

5´ Forward Primer	
SV40for1	GGAGGCCTAGGCTTTTGCAA

3´ Reverse Primer		
Gene	Sequence	Product length in bp
Id2	GCAGGCTGACAATAGTGGGA	462
Fos	GGATGATGCTGGGAACAGGA	1054
NS1	ATGTCCTGGAAGAGAAGGCA	678
Jun	TTCCTCATGCGCTTCCTCTC	912
E2F1	CAGGGTCTGCAATGCTACGA	944
ßCat	TTATGCAAGGTCCCAGCGGT	806
TAg	CACCTGGCAAACTTTCCTCA	1214
Myb	CTTCTGGAAGCTTGTGGCCA	780
Id3	ATGACAAGTTCCGGAGCGAG	453
E7	GCCCATTAACAGGTCTTCCA	404
E6	ATTCGCCCTTTTACAGCTGG	636
Bcl2	TCTGCGAAGTCACGACGGTA	440
HoxA9	GTTTAATGCCATAAGGCCGG	515
Bmi1	GGGCCATTTCTTCTCCAGGT	782
PymT	CATCTCGGGTTGGTGTTCCA	606
Core	ACTTTACCCACGTTGCGCGA	487
Oct3	GCAAAGCAGAAACCCTCGTG	846
Klf4	AAGATCAAGCAGGAGGCGGT	1084
Id1	AGAAGCACCAAACGTGACCA	980
Myc	AGTGGGCTGTGAGGAGGTTT	1001
Lmo2	TTTCCGTCCCAGCTTGTAGT	822
Nfe2L2	GCTGCTGAAGGAATCCTCAA	1008
Yap1	GCCAGGATGTGGTCTTGTTC	950
Nanog	TATGGAGCGGAGCAGCATTC	935
Sox2	CTCGCAGACCTACATGAACG	846
RhoA	AAGCATTTCTGTCCCAACGT	562
Ezh2	ACTTCGAGCTCCTCTGAAGC	1481
Gli1	CACCACATCAACAGCGAGCA	1144
v-Myc	GACACCCTGAGCGATTCAGA	1052
Suz12	TACCCTGGAAGTCCTGCTTG	769
ZFP217	CAAGAAGGGAGCACCGACAA	1188
Id4	CAGCAAAGTGGAGATCCTGC	652
Rex	GCGAGCTCATTACTTGCAGG	920

II.1.7 TEER measurement:

Barrier property of primary cells or cell lines was determined by measuring the trans-epithelial electrical resistance (TEER) as previously described (Daum et al., 2012; Srinivasan et al., 2015). Cells were placed on a heating plate at 37 °C to avoid temperature shock-related TEER fluctuation. TEER was measured with a Chopstick electrode and an epithelial voltohmmeter (EVOM) (World Precision Instruments, Sarasota, USA). For measuring TEER of ALI cultured cells the cells were set up to LLC conditions 2 hours prior measurement and returned to ALI afterwards.

II.1.8 Histology and light microscopy

Light microscopic images of hAEpC cells, transfected cell populations and hAELVi cells grown either on cell culture plates or Transwell® membranes were acquired with a Zeiss light microscope (Zeiss Imager M1m, Zeiss, Germany), using a 10x or 20x objective. For histological cross sections hAEpC cells and hAELVi cells previously grown on Transwell® filters were fixed on days 7 and 14 with 3% paraformaldehyde (PFA) for 30 min at room temperature. Afterwards, the samples were dehydrated with an ethanol dehydration row (35-50-70-95-95-100% for 10 min each), followed by a treatment with Histoclear II (Histological Clearing Agent-Fa. National diagnostics) for 10 min. Subsequently the samples were embedded in paraffin (Histowax Embedding Medium-Leica Microsystems) for one hour, stored at 4°C overnight, and were cut the other day in 4 µm slices using a Microtom-Reichert Jung 2040 Autocut. In a next step the slices were stained with hematoxylin/eosin and analyzed with a Zeiss light microscope (Zeiss Imager M1m, Zeiss, Germany), using a 100x objective. Image acquisition and analsysis as performed with the Zeiss ZEN 2012 software.

II.1.9 Confocal laser scanning microscopy

hAEpC cells and hAELVi cells were grown on Transwell® membranes with a pore size of 0.4 µm and growth area of 1.12 cm^2 (3460, Corning) for seven and 14 days, under LLC and ALI conditions, as described previously or grown on cell culture chamber slides for 14 days.

ZO-1 staining: Samples were then fixed with 3% PFA in phosphate buffered saline (PBS) for 30 min at room temperature. Afterwards, the samples were quenched with 50 mM NH_4Cl/PBS for 10 min, subsequently blocked and permeabilized using a mixture of 0.5% bovine serum albumin(BSA)/0.025% Saponin/PBS for 30 min at room temperature. The primary antibodies against ZO-1 (rabbit anti-ZO-1, Catalog No 61-7300, Invitrogen) were diluted 1:200 in 0.5%BSA/0.025% Saponin/PBS and

incubated at 4 °C overnight. The secondary antibodies ZO-1 (polyclonal Alexa-Fluor 633, conjugated goat anti-rabbit, Catalog No. A21070, Invitrogen) were diluted in PBS (1:400) and incubated for one hour at 37 °C. The samples were washed with PBS and counterstained with DAPI (1:50,000). Transwell® membranes were then mounted in DAKO mounting medium (Product No. S302380-2, DAKO), as previously described in de Souza Carvalho *et al.* (de Souza Carvalho et al., 2011), and analyzed by confocal laser scanning microscopy (Zeiss LSM710, Zeiss, Germany). Microscopic images of fixed samples were acquired at 1024×1024 resolution, using 63X water immersion objective and z-stacks of around 6 µm. Confocal images were analyzed using Zen 2012 software (Carl Zeiss Microscopy GmbH) and Fiji Software (Fiji is a distribution of ImageJ available at http://fiji.sc).

Occludin and CD326 staining: Cells were fixed with -20°C cold Methanol for 10 minutes at 4°C and afterwards were washed three times with phosphate buffered saline (PBS) for 5 minutes each to rehydrate the cells. The cells were blocked with 0.5% bovine serum albumin (BSA) in PBS for 30 minutes at room temperature. Afterwards the cells were washed again three times with PBS to remove unbound BSA. The antibodies against EpCAM (CD326) are directly FITC-labeled and were used in a concentration of 1 µg/ml diluted in PBS/0.5%BSA/0.1%Tween80. Incubation took place for 1 hour at 37°C. The primary antibodies against Occludin (Mouse anti-Occludin Catalog No 33-1500, Invitrogen) were unlabeled and used in a concentration of 1 µg/ml diluted in PBS/0.5%BSA/0.1%Tween80. Incubation with primary antibodies took place overnight at 4°C. The secondary polyclonal FITC-labeled antibody (Polyclonal Goat Anti-Mouse Immunoglobulins/FITC, Catalog No F0479, Dako Cytomation) was used in 1:400 dilution for 1 hour at 37°C after removal of the primary antibody by three times washing the cells with PBS and a further blocking step. The cell nuclei were counterstained with DAPI (1:50,000) and mounted in FluorSave reagent (Catalog No 345789, Merck Millipore, Darmstadt, Germany). Pictures were taken with a laser-scanning confocal microscope (Zeiss LSM710, Zeiss, Germany). Acquisition and analysis was performed with Zen 2012 software (Carl Zeiss Microscopy GmbH).

II.1.10   Scanning electron microscopy (SEM)

SEM images were taken with a Zeiss SEM EVO® HD15 (Zeiss, Germany) under high pressure conditions with a secondary electron detector and using 10 kV acceleration voltage. hAELVi cells (passage 41) on Transwell® filters were fixed after 8 days in culture, either in ALI and LLC, in 200 mM HEPES buffer containing 1% glutaraldehyde at 4°C, overnight. The following day, cells were washed twice for 10 min in HEPES buffer and dehydrated with gradual ethanol concentrations (50-60-70-80-90-96-99-100% for 20 min each). The filters were then sputtered with gold and examined with the SEM.

II.1.11   Transmission electron microscopy (TEM)

hAELVi cells (passages 36) were grown on Transwell® membranes, under LLC and ALI conditions for 12 days. Thereafter, the samples were processed as described in Susewind *et al.* (Susewind et al., 2015), with minor modifications. Briefly, the membranes were fixed with a 1% glutaraldehyde solution in SAGM for five minutes at 37°C, followed by incubation with 1% glutaraldehyde in 200 mM HEPES buffer, pH 7.4, overnight at 4°C. Afterwards Transwell® inserts were put in a 50 ml falcon tube filled with HEPES buffer, and sent to our collaborators Dr. Urska Repnik and Prof. Dr. Gareth Griffiths from Oslo University, Denmark, for further preparation. For epon embedding the samples were postfixed with 2% OsO_4 (EMA, PA, USA) solution containing 1.5% potassium ferricyanide for one hour on ice, and stained *en bloc* with 1.5% aqueous uranyl acetate (EMS, PA, USA) for 30 min. Cells were then dehydrated at room temperature using a graded ethanol series (70-80-90-96-(4x)100% for 10 min each), progressively infiltrated with epoxy resin (50-75-100%)(Sigma-Aldrich; St.Louis/MO, USA). Transwell® membranes with cells were flat embedded and blocks were polymerized overnight at 70°C. Ultrathin sections of 70-80 nm, perpendicular to the filter plane, were cut with a Leica ultramicrotome Ultracut EM UCT (Leica Microsystems, Austria) using an ultra-diamond knife (Diatome, Switzerland) and examined with a CM100 transmission electron microscope (FEI, The Netherlands). The images were recorded digitally with a Quemesa TEM CCD camera (Olympus Soft Imaging Solutions, Germany) and iTEM software (Olympus Soft Imaging Solutions, Germany).

II.1.12   mRNA isolation and semi-quantitative rtPCR

Relative changes in mRNA transcription of lung cell-specific marker proteins CAV-1, SP-C and AQP-5 were determined using semi-quantitative real-time polymerase chain reaction (rtPCR). Total RNA of hAELVi cells was collected on day 14 of cell culture on six-well plates, freshly isolated ATII cells, and ATI-like hAEpCs, previously grown on Transwell® filters for eight days. RNA was extracted with QIAshredder (Qiagen, Hilden, Germany) and RNeasy Mini kit (Qiagen, Cat.No. 74106) according to the manufacturer's protocol. RNA amount was measured using a photometer (Eppendorf, Hamburg, Germany). A 1 µg amount of RNA was then reverse transcribed into cDNA with a QuantiTect Reverse Transcription kit (Qiagen, Cat.No. 205314). The primers for reaction were constructed and ordered from Eurofins. Sequence of primers and probes are presented in Table II-2. Semi-quantitative real-time PCR was performed with QuantiTect Sybr Green PCR kit (Qiagen, Cat.No. 204143). Run information: seven min 95°C; 40 cycles of ten sec 95°C, 30 sec 65°C, 30 sec 72°C; and one min 65°C in a Bio-Rad CFX96 real-time PCR machine. Glyceraldehyde 3-phosphate dehydrogenase (GADPH) was used as the internal control to correct for variations in the cDNA content among the samples. The data were normalized to the GADPH expression levels and were presented as the average from three independents experiments. The relative gene expression levels were calculated using the comparative Ct ($\Delta\Delta$Ct) method(Livak and Schmittgen, 2001). Data analysis was performed with the Bio-Rad CFX Manager software.

Table II-2: Primers for lung cell-specific marker semi-quantitative rtPCR

Marker		nucleotide sequence (5' → 3')	Product length in bp
AQP5	forward	CCTACCATCCTGCAGATCGCGC	210
	reverse	TGCCACACCGTAGAGGATGCCA	
SP-C	forward	AAGCCCGCAGTGCCTACGTCTA	273
	reverse	TGGATGACCCCGCTTCAGTGGA	
CAV-1	forward	ACAGTTTTCATCCAGCCACGGGC	202
	reverse	GGTGTTTAGGGTCGCGGTTGACC	
GAPDH	forward	GGAGAAGGCTGGGGCTCATTTGC	364
	reverse	CCCGTTCAGCTCAGGGATGACCT	

II.1.13   Transport studies

To evaluate the transport of sodium fluorescein (FluNa) across the monolayers, hAELVi.A cell (1×10^5 cells/cm²) were seeded on fibronectin/collagen-coated Transwell® membranes with a pore size of 0.4 µm and a growth area of 1.12cm² (3460, Corning). The cells were cultured under LLC and ALI, respectively, and TEER measurements were performed every other day for 14 days. Transport experiments were then performed according to Elbert *et al.* (Elbert et al., 1999) with minor modifications. Briefly, before the cells were washed twice with pre-warmed Krebs-Ringer Buffer (KRB; NaCl 142.03 mM, KCl 2.95 mM, K_2HPO_4*$3H_2O$ 1.49 mM, HEPES 10.07 mM, D-Glucose 4.00 mM, $MgCl_2$*$6H_2O$ 1.18 mM, $CaCl_2$*$2H_2O$ 4.22 mM; pH 7.4) and incubated in KRB for 45 min. After measuring the TEER, the medium was aspirated and 520 µL FluNa (10 µg/ml in KRB) ± 16mM EDTA were added to the apical compartment (donor) and 1.7 mL KRB were added to the basolateral compartment (acceptor). Directly after adding the solutions, samples were taken from the donor (20 µL) and the acceptor (200 µL), respectively, and transferred into a 96-well plate. Afterwards, the plates were placed on a MTS orbital shaker (150 rpm; IKA, Germany) in the incubator and samples were taken every 30 min for three hours. Taken volumes were refilled with 200 µL KRB. At the end of the experiment the TEER was measured again and the samples in the 96-well plate were measured with a Tecan® plate reader using wavelength of 488 nm (em) and 530 nm (ex).

II.1.14   Statistical analysis:

Data are representative from 2-3 experiments and show as mean ± SEM. P values were determined using an unpaired two-tailed Student's t-test assuming equal variances of all experimental datasets using Microsoft Excel software. Two-way ANOVA with Bonferroni´s posttest was performed using GraphPad Prism 5 software (GraphPad).

II.2 Results

In the following the results of the immortalization (II.2.1) of hAEpC resulting in the new cell line hAELVi, the TEER value analysis of said models (0), the morphological analysis of hAELVi cells (II.2.3), rtPCR of lung-specific markers (0) and transport of sodium fluorescein through hAELVi cell monolayers (II.2.5) is presented. Mainly the results highlight the characterization of the new hAELVi cell line, but cover also some previous work regarding other transfected cell populations and the primary model of alveolar epithelial type I cells (hAEpC).

II.2.1   Immortalization

II.2.1.1 Transfection with lentiviral vectors and propagation of infected cells

Transfection of hAEpC was achieved with lentiviruses carrying different vectors with transformation genes. The abbreviations of these vectors are explained in Table II–3, as well as the transformation genes they are carrying. To infect the different isolations of hAEpC mixtures of different lentiviruses were used as shown in Table II–3 to Table II–6.

Table II-3: Abbreviations and explanation of the vectors used for infection of hAEpC.

Abbreviation of vector	Explanation
NA	New All Mix of 33 different lentiviral vectors with each one transforming gene from the "mild proliferator" group under the control of the constitutive simian virus 40 (SV40) promoter
pLentitert	Lentiviral vector with human telomerase gene *hTert* under the control of the constitutive SV40 promoter
pJSARLT	Lentiviral vector with the *Large T-Antigen* under the translational control of an autoregulated transactivator tet-dependent system
pJSCMVTA2	Vector with transactivator gene under the control of the constitutive cytomegalovirus (CMV) promoter
pJSARTA3	Vector with transactivator gene under the control of autoregulated transactivator tet-dependent system
8cG	Mix of vectors with eight different constitutively expressed transforming genes ("mild proliferators") under either the translational control of the SV40 or the CMV promoter. Transformation genes in the mixture: *ID1, ID3, E6, E7, EZH-2, Lmo2, core, Nanog*
pJStetID1/pJStetID3/pJStetE6	Lentiviral vector with the *ID1, ID3* or *E6* gene, respectively, under the translational control of a transactivator-dependent promoter system. The tet-dependent transactivator is expressed (either constitutively or autoregulated) from another vector (pJSCMCTA2 or pJSARTA3)
pJSGFP	Constitutively expressed GFP as transfection control

None of the cell pools that were obtained by the infection of hAEpC from isolation "hips59" with different mixtures of lentiviruses, which are listed in Table II-4 could be propagated further than passage 10.

Table II-4: Infections of hAEpC from isolation "hips 59".

The different mixtures of lentiviruses used to infect hAEpC "hips 59" are listed here. None of the transfected cell pools could be propagated further than passage 10.

Vector/Mix of vectors	Died after passage x	Frozen in passage x or still in culture
NEG b	6	---
NA1	5	---
NA2	5	---
NA3	5	---
JSARLT+Lentitert 1	5	---
JSARLT+Lentitert 2	5	---
JSCMVTA2+JStetID1/ID3/E6a	6	---
JSCMVTA2+JStetID1/ID3/E6b	6	---
JSCMVTA2+JStetID1/ID3/E6c	7	---
JSCMVTA2+JStetID1/ID3/E6d	5	---
JSCMVTA2+JStetID1/ID3/E6e	6	---
JSCMVTA2+JStetID1/ID3/E6f	6	---
JSCMVTA2+JStetID1/ID3/E6g	8	---
JSARTA3+JStetID1/ID3/E6a	10	---
JSARTA3+JStetID1/ID3/E6b	7	---
JSARTA3+JStetID1/ID3/E6c	7	---
JSARTA3+JStetID1/ID3/E6d	8	---
JSARTA3+JStetID1/ID3/E6e	7	---
JSARTA3+JStetID1/ID3/E6f	8	---
JSARTA3+JStetID1/ID3/E6g	4	---
JSARTA3+JStetID1/ID3/E6h	4	---
JSARTA3+JStetID1/ID3/E6i	7	---
JSARTA3+JStetID1/ID3/E6j	2	---
JSARTA3+JStetID1/ID3/E6k	4	---

Some of the transfected cell pools from the hAEpC isolation "hips62", which are listed in Table II-5, could be propagated further than passage 6 up to passage 19 and were cryo-preserved to conserve them for later studies.

The transfections JSARLT+Lentitert2, JSCMVTA2+JStetID1/ID3/E6b, JSARTA3+JStetID1/ID3/E6d, 8cGb and 8cGe were examined regarding their ability to develop TEER (see Figure II-23 and Figure II-24).

Table II-5: Infections of hAEpC from isolation "hips 62".
The different mixtures of lentiviruses used to infect hAEpC "hips 62" are listed here. Some of the transfected cell pools could be propagated further than passage 6 up to passage 19, but did not develop TEER value (Figure II-23 and Figure II-24) and because of that were frozen to conserve them for later studies.

Vector/Mix of vectors	Died after passage x	Frozen in passage x or still in culture
NEG a	3	---
NEG b	4	---
NA 1	4	---
NA 2	5	---
JSARLT+Lentitert 1	4	---
JSARLT+Lentitert 2	---	7
JSARLT+Lentitert 3	4	---
JSARLT+Lentitert 4	4	---
JSCMVTA2 + JStetID1/ID3/E6a	4	---
JSCMVTA2 + JStetID1/ID3/E6b	---	6
JSCMVTA2 + JStetID1/ID3/E6c	4	---
JSCMVTA2 + JStetID1/ID3/E6d	5	---
JSARTA3+ JStetID1/ID3/E6a	4	---
JSARTA3+ JStetID1/ID3/E6b	4	---
JSARTA3+ JStetID1/ID3/E6c	5	---
JSARTA3+ JStetID1/ID3/E6d	---	6
8cGa	---	9
8cGb		19
8cGc	5	---
8cGd	5	---
8cGe	7	---
8cGf		14
8cGg		19
8cGh	4	---

The different mixtures of lentiviruses used to infect hAEpC "hips 63" are listed in Table II-6. The hAELVi cell line, which could be propagated up to passage 75 and is still in culture, emerged from the infection with the New All called mixture of 33different lentiviruses carrying 33 different transformation genes (NA1). This work focusses mainly on this cell line due to its immortal lifespan and ability to form an ATI-like functional barrier. The cell pool obtained by infection with NA2 did not exhibit TEER and was cryo-preserved to save the cell material for later investigations.

Table II-6: Infections from hAEpC isolation "hips 63".
The different mixtures of lentiviruses used to infect hAEpC "hips 63" are listed here. The hAELVi cell line emerged from the infection NA1 and is still in culture in passage 75.

Vector/Mix of vectors	Died after passage x	Frozen in passage x or still in culture
NA1		**Still in culture:** **passage > 75** **hAELVi cell line emerged** **from this infection**
NA2	---	11
JSARLT lentitert 1	7	---
JSARLT lentitert 2	7	---
JSARLT	9	---
lentitert	9	---

II.2.1.2 Growth curve of hAELVi

The hAELVi cell line previously consisted of three cell clones, which were able to exhibit TEER and emerged from the infection of hAEpC isolation "hips 63" with the NA1-called mixture of lentiviruses carrying 33 different transformation genes (see Table II–1, Table II–3 and Table II–6): hAELVi.A, hAELVi.B and hAELVi.C.

Figure II-1 shows the growth curve of the immortalized cell lines in passage 18. hAELVi cell lines showed a sigmoidal growth curve, with a lag phase after seeding, developing into an exponential growth phase and ending in a stationary phase.
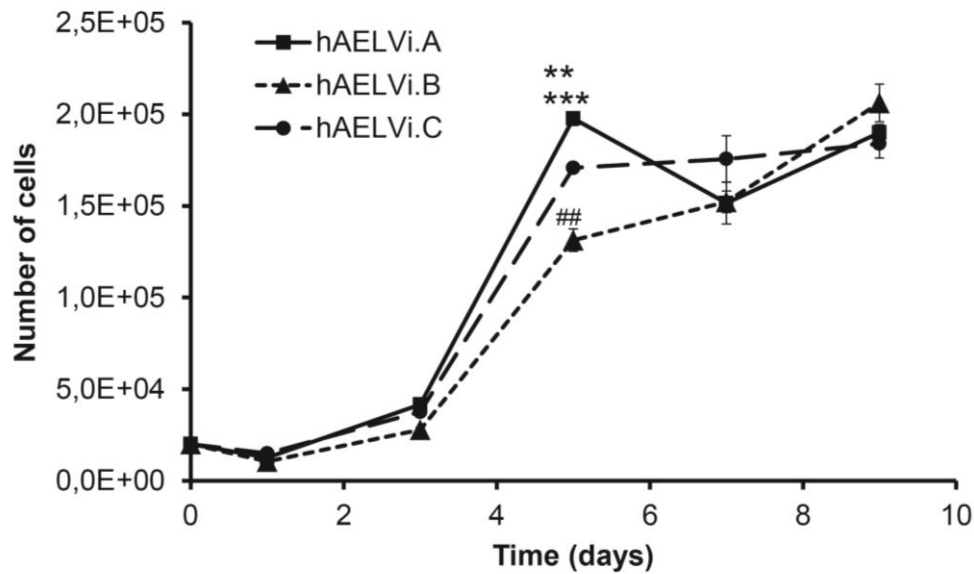
Figure II-1: Growth curve of hAELVi cells.
Growth curve of immortalized lines (hAELVi.A, hAELVi.B and hAELVi.C), grown in 24-well cell culture plates, passage 18, for 9 days. Data shown are mean ± SEM (n=3); ***$P<0.001$vs. hAELVi.B; **$P<0.01$ vs. hAELVi.C; ##$P<0.01$ vs. hAELVi.C

After passage 20 cell clone hAELVi.C was excluded from further analysis, because the cells lost their ability to develop TEER values (see Figure II-8)

II.2.1.3 PCR for viral genes on genomic DNA

The hAELVi cells were seeded on Transwell® filters (0.4µm) and afterwards cultivated in six-well cell culture plates to characterize the integrated genes. The primers used to detect the integrated genes are listed in Table II-1. PCR analysis of the immortalized cell lines demonstrated integration of 7 genes - *Id2, Id3, E7, Bcl2, Core, Myc* and *Nanog* (Figure II-2). The agarose gel depicted in Figure II–2 shows the PCR of hAELVi.A, passage 29. The result for hAELVi.B looked identically (data not shown).
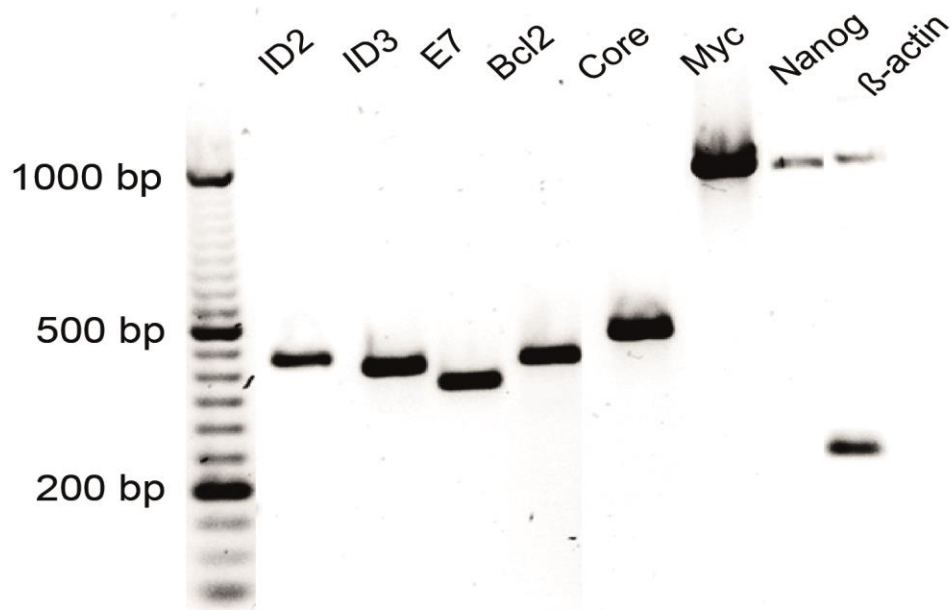
Figure II-2: PCR analysis of transformation genes.
PCR of viral genes on genomic DNA of hAELVi.A, passage 29, after lentivirus mediated transfection with immortalizing genes. From 33 genes used, seven were identified: *ID2, ID3, E7, Bcl2, Core, Myc* and *Nanog.*

II.2.1.4 Chromosomal analysis for ploidy variations

Genomic DNA from hAELVi cells was investigated for ploidy variation with the Affymetrix Cytoscan HD array. The experiments were carried out by Ulrike Fischer from the Institute of Human Genetics, University Hospital of Saarland University, Homburg /Saar, Germany under the direction of Prof. Eckart Meese.

In brief, 13 chromosomes revealed no alterations in copy number, in neither earlier nor late passage. The remaining chromosomes revealed several deleted or duplicated chromosome regions. Figure II-3A shows the karyotype analysis of hAELVi.A and hAELVi.B, both at passage 19. The pink rows next to each chromosome visualize the two chromosomes of hAELVi.A, the purple ones the two chromosomes of hAELVi.B, respectively. Loss of a chromosome region is indicated as red sign and duplication of a chromosome region is indicated as blue sign. In hAELVi.A cells one of chromosomes 1, 4, 9, 11 and 16, and both of chromosomes 6 lost chromosomal regions, while one of chromosomes 2, 4, 5, and 15, and both of chromosomes 14 an 17 gained parts through duplication of chromosomal regions. hAELVi.B lost parts of one of chromosomes 1, 4, and 16, and of both chromosomes 6 and 11. Duplications could be found in one of chromosomes 2, 4, 5, 14, 16, and 17, and in both of chromosomes 15. To investigate whether the chromosome profile of the hAELVi cells changed over time a later passage was also examined regarding its

karyotype. Figure II-3B shows the chromosome profiling of hAELVi.A at passage 43. Here the two purple lines next to the chromosome represent the two chromosomes, respectively. The chromosomal profile changed compared to passage 29. Chromosome 1, which already lost a part in the outer region of the p-arm, gained regions in the q-arm. Chromosome 4 showed additional loss and Chromosome 5 additional gain in the second chromosome. Chromosome 6 also gained chromosomal parts through duplication in both chromosomes, as well as chromosomes 7, 9, 12, and 20.
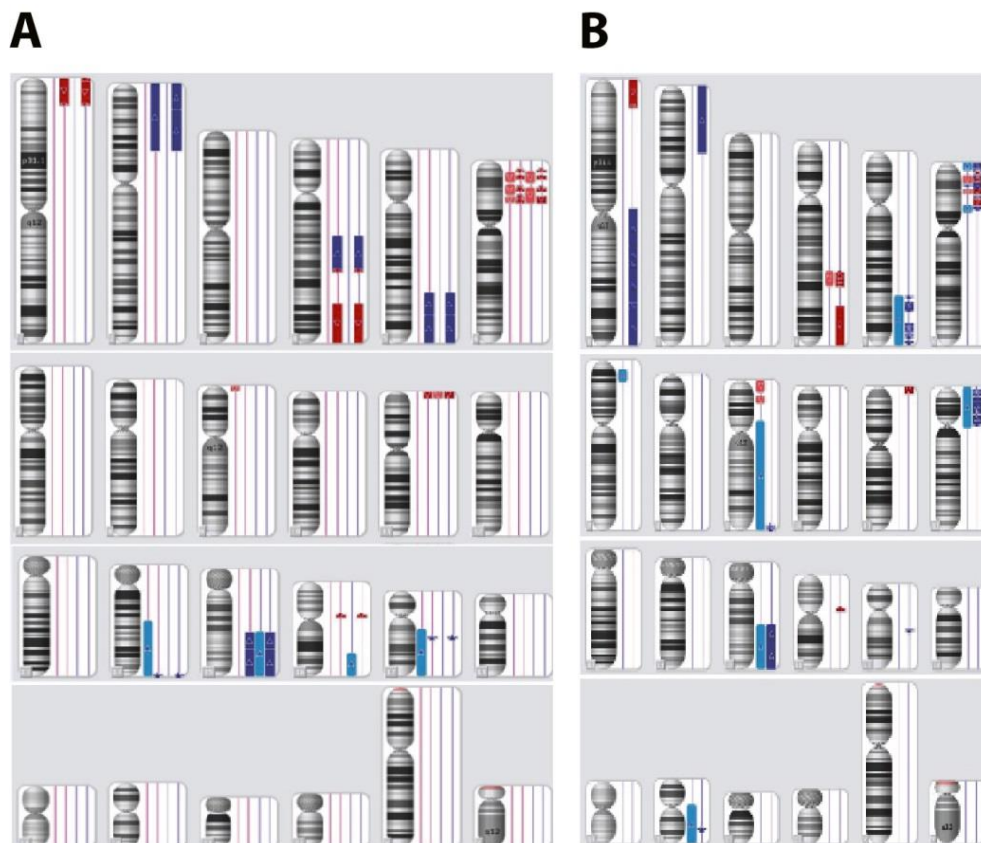
Figure II-3: Karyotype analysis
Chromosome profiling was performed with Affymetrix Cytoscan HD array. A: Chromosome profiling showing an overview on the karyotype at cell culture passage 19 is presented: hAELVi.A (pink, first two rows) and hAELVi.B (purple, last two rows). B: Chromosome profiling of hAELVi.A at passage 43 Loss of a chromosome region is indicated as red sign and duplication of a chromosome region is indicated as blue sign. Row 1 left to right: 1, 2, 3, 4, 5, 6; row 2 left to right: 7, 8, 9, 10, 11, 12; row 3 left to right: 13, 14, 15, 16, 17, 18; and row 4 left to right: 19, 20, 21, 22, X, and Y.

II.2.2 TEER measurements

The transepithelial electrical resistance is a measure of the integrity and tightness of the cell monolayers. The aim of this work was to generate an alveolar cell line with barrier properties reflecting the hAEpC model and hence the *in vivo* situation in the alveolus. The following section shows the results from the TEER measurements of the hAEpC model and the new hAELVi cells under different culture conditions.

All measurements were carried out by me, except the measurements of hAELVi cells at passages higher than number 36. Those were carried out by Stephanie Kletting, as well as the measurement of hAELVi cells in Figure II-9C.

II.2.2.1 The TEER of the hAEpC model

As mentioned in I.2.1 the TEER of the hAEpC model reaches values of 1000 to 2000 Ω*cm^2 during a time span of 14 days. The maximum TEER can be measured between days 8 to 10 of culture. Nevertheless due to the quality of the lung material, inter-individual differences and the patient's case history, the TEER of different isolations can vary strongly, as visible in Figure II-4 where TEER curves of 10 different hAEpC isolations are plotted. 50% of the isolations, namely isolations "404", "407", "409", "410", and "412", barely exhibit any TEER and hence are not usable for experiments. The remaining 5 isolations develop high TEER values. Isolation "405" shows very high TEER and a prolonged life-span, so that its suitability for experiments is questionable. Isolations "401", "403", "406", and "408" show the expected behavior of the hAEpC model regarding the development of TEER.
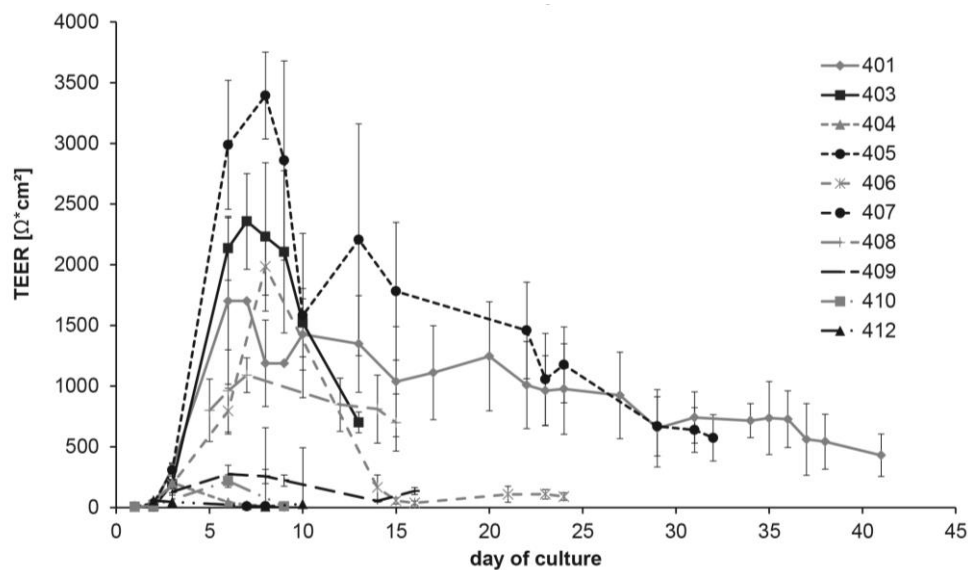
Figure II-4: TEER curves of 10 different hAEpC isolations.
Cells were cultured on Transwell® filter (0.4 µm pores) and TEER was measured depending on isolation number between 3 and 41 days. Data shown are mean ± SD (n=12)

II.2.2.2 TEER of cell pool "NA1"

Cells from infection of hAEpC "hips63" with the transfection mixture New All 1, comprised of 33 different transformation genes under the control of the constitutively expressed SV40 promoter were seeded on Transwell® filter in passage 10 and TEER was measured for 15 days. Figure II-5 shows the TEER curve of every single Transwell® filter. Filters 4, 5, and 6 developed high TEER between 189 $\Omega*cm^2$ and 830 $\Omega*cm^2$, whereas filters 1, 2, and 3 did not develop high TEER values. To save and further propagate the TEER developing cell pools, the cells were mildly detached from the filter with trypsin and seeded into a well of a 96-well cell culture plate. From there the 3 different cell populations were maintained and transferred to a well of a cell culture plate with bigger diameter once they reached confluence. Later on the three cell populations were named hAELVi.A, hAELVi.B and hAELVi.C and used in all further experiments described in this work.
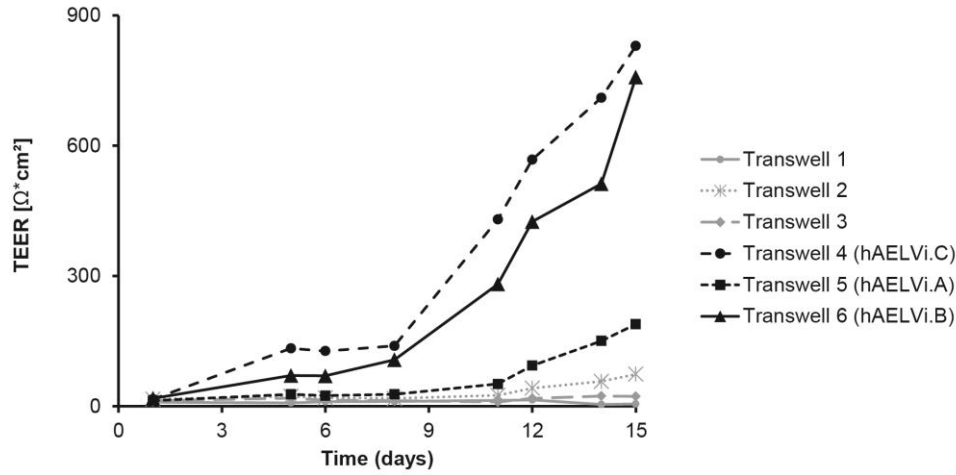
Figure II-5: TEER of cell pool "NA1"

Cells from transfection of hAEpC "hips63" with the transfection mixture New All 1 were seeded on Transwell® filter in passage 10 and TEER was measured for 15 days. The cell populations from Transwell® filter 4, 5, and 6 were transferred to cell culture plastic and further propagated.

II.2.2.3 The TEER of the immortalized cell lines hAELVi.A and hAELVi.B

II.2.2.3.1 TEER of hAELVi cells compared to hAEpC cells

While The hAEpC developed a TEER of a maximum 2000 Ω*cm^2 around day six to eight, followed by a subsequent decline of TEER value, demonstrating a short lifespan of around 15 days, a typical behavior for primary cells (Daum et al., 2012; Fuchs et al., 2003), the TEER of the two hAELVi clones A and B depicted in the same graph reached a TEER of 2000 Ω*cm^2 six to ten days later, which was conserved for up to 25 days. Figure II-6 shows the course of TEER of hAELVi.A and hAELVi.B , both passage number 36, over a time span of 28 days and the TEER of hAEpC isolation "403" over 13 days. hAELVi.A shows a faster set on of TEER, with values of almost 1000 Ω*cm^2 as early as on day 3 of culture, compared to hAELVi.B, which reaches equal high values around day 10 of culture.
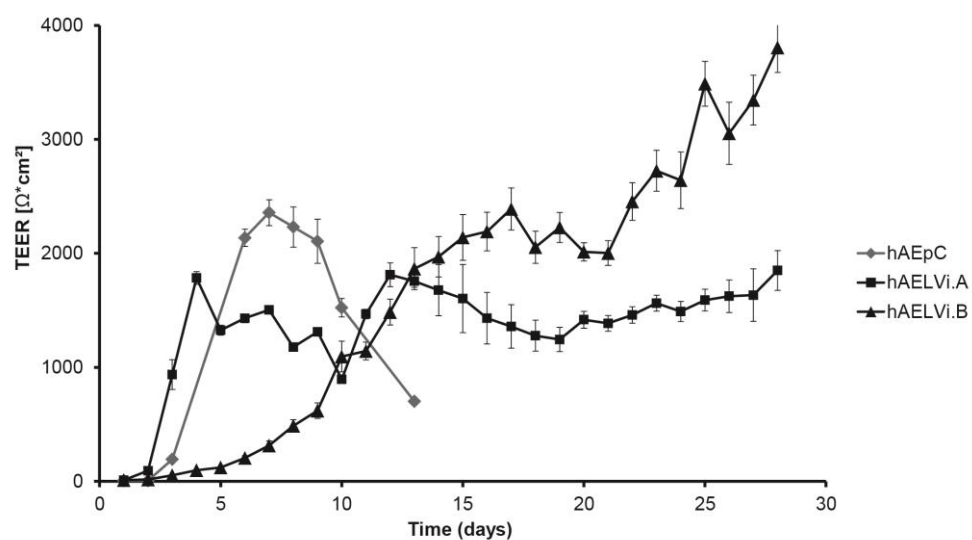
Figure II-6: TEER of hAELVi.A and hAELVi.B cells compared to hAEpC cells
Comparative TEER curve of immortalized cells hAELVi.A and hAELVI.B, both in passage
36, and primary ATI-like cells (hAEpC), growing on Transwell® membranes. Data shown are
mean ±SEM

II.2.2.3.2 The TEER of hAELVi cells in different passages

Figure II-7 shows the TEER curves of hAELVi.A at different passages from number 21 up to number 72. hAELVi.A conserved its ability to develop high TEER values.
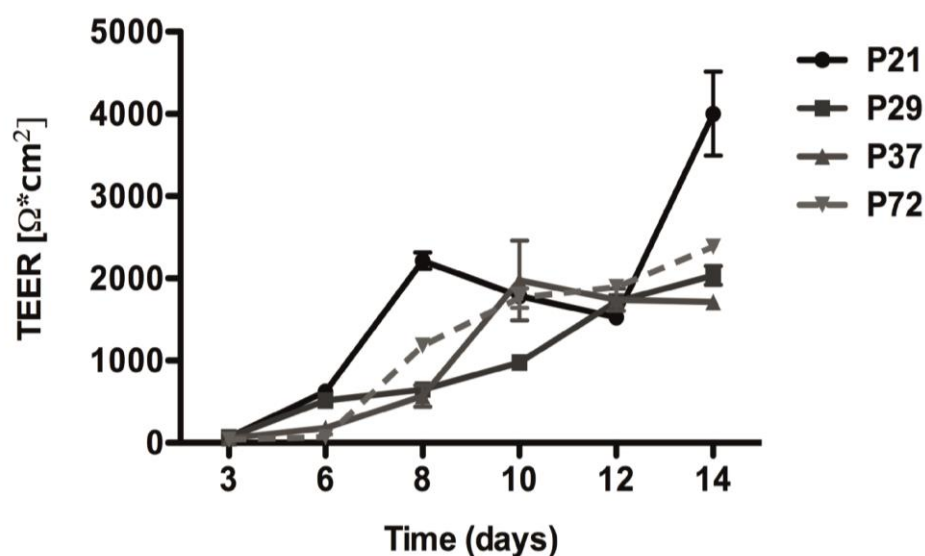
Figure II-7: TEER of hAELVi.A.
TEER curves of different passages of hAELVi.A cells during 14 days in culture. Data shown are mean $\pm$ SEM (n=3).

The maximum TEER values of the immortalized hAELVi cells, as well as the primary hAEpC model, reached during a culture time of 15 to 30 days are shown in Figure II-8. The immortalized cell lines hAELVi.A and hAELVi.B conserved their ability to develop high TEER values, up to 2000 to 3000 Ω*cm^2, even very high TEER values up to 4000 Ω*cm^2 were observed, while the hAELVi.C cell line lost its ability to form a barrier after passage number 18 and was hence excluded from further investigations.
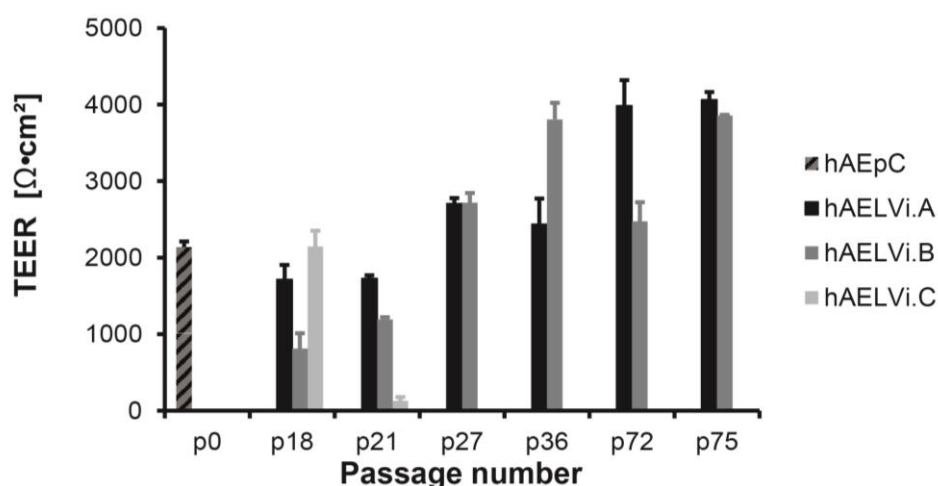
Figure II-8: Maximum TEER values.
TEER measurement of immortalized cells hAELVi.A, hAELVi.B and hAELVi.C in different passages, after 15 to 30 days in culture, compared to primary ATI cells cultivated for 15 days in culture. Shown is a mean of maximum TEER value reached during culture. Data shown are mean $\pm$ SEM (n=3)

II.2.2.3.3 TEER in different culture conditions: air-liquid interface culture compared to liquid-liquid culture

TEER measurement of hAEpC cells from isolations "hips 40" and "hips 41" and hAELVi.B grown for 14 days on Transwell® filter in either air-liquid interface culture (ALI) or liquid-liquid culture (LLC) conditions revealed significant differences depending on the respective culture. LCC conditions resulted in significant higher TEER for hAEpC cells compared to ALI conditions (Figure II-9A and B). Even though hAEpC "hips 40" developed lower TEER at all compared to "hips 41", the tendency is the same. The very reverse observation could be made with hAELVi.B cells (Figure II-9C), where ALI conditions caused the monolayer to develop significant higher TEER compared to LLC conditions.
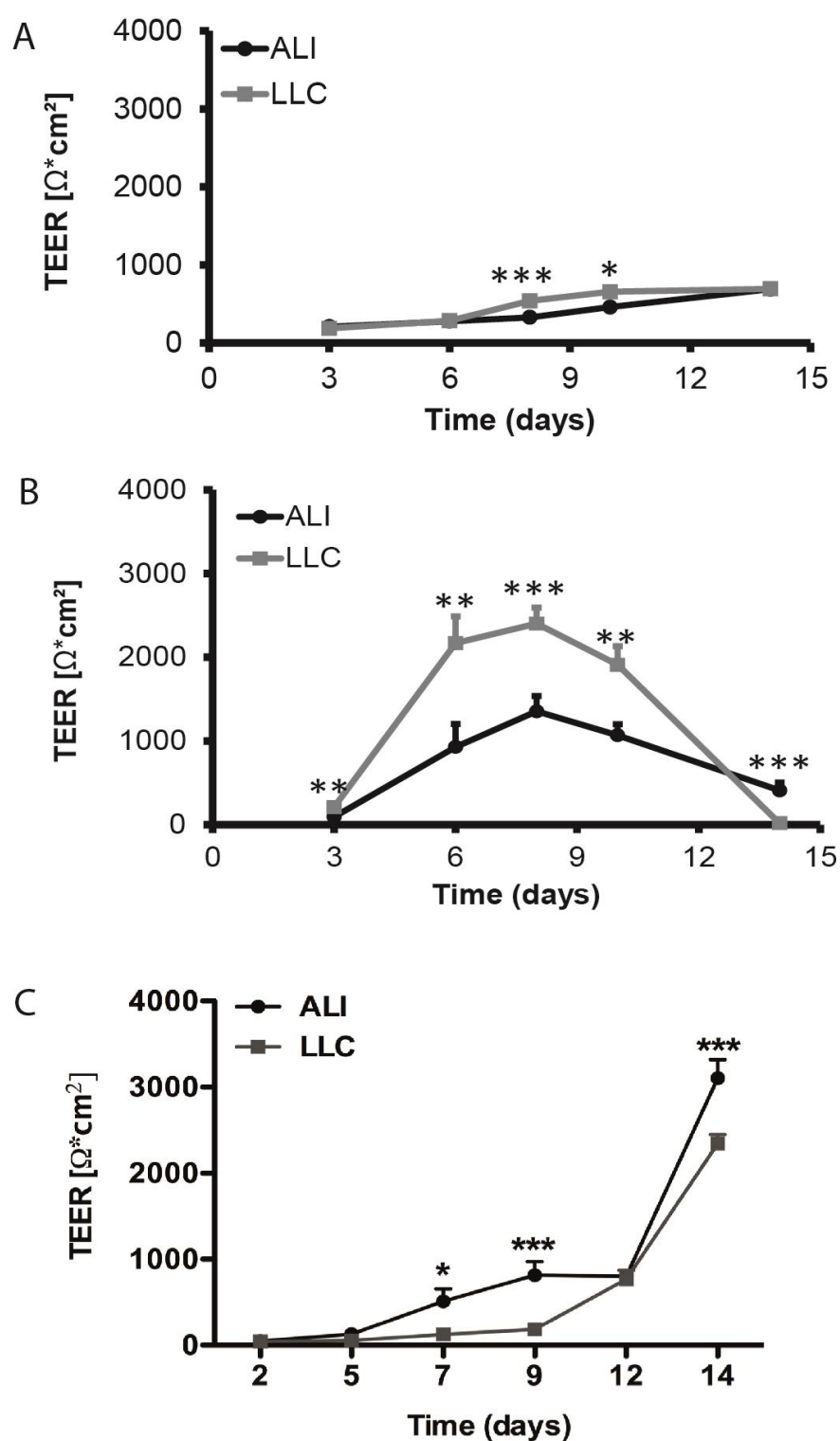
Figure II-9: TEER of air-liquid interface culture compared to liquid-liquid culture.
TEER measurement of hAEpC cells from isolations "hips 40" (A) and "hips 41" (B) and hAELVi.B (C) grown for 14 days on Transwell® filter in either ALI (black) or LLC (grey) conditions. Data shown are mean ± SEM. *P<0.05; **P<0.01; ***P<0.001

II.2.3 Morphology

The morphology of the new immortalized cell lines hAELVi.A and B, and for the purpose of comparison from other transfected cell lines and the hAEpC model, are presented in this section. Acquisition of light microscopic images and SEM images was performed by me, as well as the sample preparation. Staining of hAELVi cells with immunofluorescence-labeled anti-ZO1 antibodies and image acquisition were performed by Stephanie Kletting and Cristiane de Souza Carvalho-Wodarz, all other CSLM images and the respective sample preparations I performed by myself. The histological cross sections were prepared by Stephanie Kletting and Marijas Jurisic, or by me and Leon Muijs. The TEM images were performed by Urska Repnik at the Department of Biosciences, University of Oslo, under the direction of Gareth Griffith.

II.2.3.1 Light microscopy analysis

The transfected cell population "NA1", which later results in the immortalized hAELVi cell lines, showed in early passages (numbers 3 and 6) a very similar morphology to "JSARLT+Lentitert2" and "JSARTA3 ID1/ID3/E6d": flat wide cells forming contact-inhibited monolayers. Compared to passage 3 (Figure II-10A), the NA1 cell pool looked more homogenous in passage 6 (Figure II-10B)
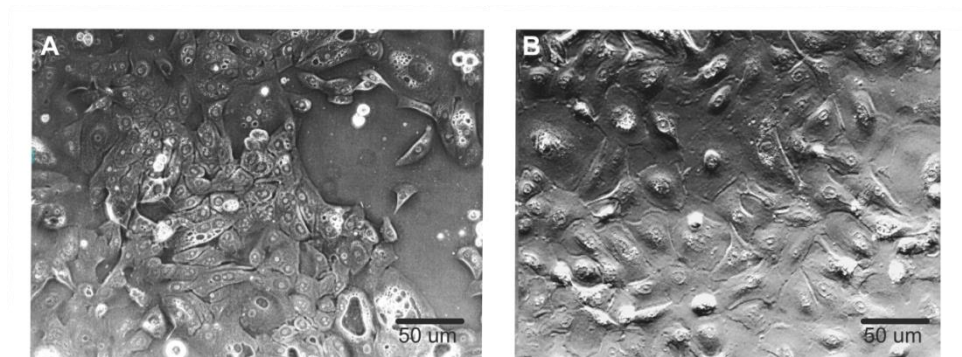
Figure II-10: Light microscopic images of "63NA1" in early passages.
Cell population "63NA1" seeded on cell culture plates. Passage number 3(A) looks less homogenous than passage 6 (B). Magnification 100x.

The three hAELVi cells lines A, B and C resulted upon splitting of the polyclonal cell population "63NA1" and their morphology as observed through the light microscope demonstrates Figure II-11. The three different lines do not differ in morphology, the cells are similar in shape and size and show contact inhibited growth forming a monolayer. Compared to earlier passages (see Figure II-10) the cells appear smaller, and not quite as flat as before.
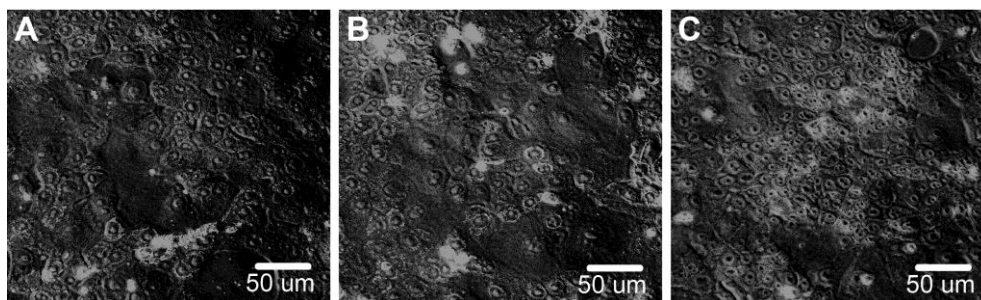
Figure II-11: Light microscopic images of hAELVi cells.
The cell lines hAELVi.A (A), hAELVi.B (B) and hAELVi.C (C) grown on cell culture plates to almost confluence. Passage number 18. Magnification 100x.

Seeded on Transwell® filter the hAELVi cells also form contact-inhibited monolayers, but appear more densely packed as when grown on cell culture plates. Figure II-12 shows the hAELVi.A and B cell lines in passage 36 and for comparison hAEpC cells. The hAEpC cells seem to be bigger than the hAELVi cells.
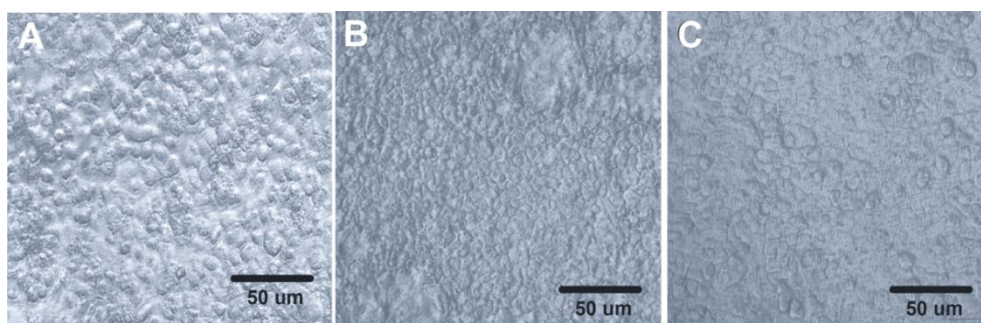
Figure II-12: Comparison of hAELVi cells and hAEpC cells on Transwell® filter.
hAEpC cells (A), hAELVi.A (B) and hAELVi.B (C) cells grown on Transwell® filter (0.4 μm pores, liquid-liquid culture) on day 7 of culture. Immortalized cells are passage 36. Magnification 100x.

The observation of histological cross sections of hAELVi cells and hAEpC cells cultured on Transwell® filters for seven days under liquid-liquid culture conditions confirms the assumption that both cell types differ in morphology. Figure II-13A shows the very thin cell body of the primary squamous epithelial cells, while the immortalized cells, depicted in Figure II-13B feature a rather cuboidal shape.
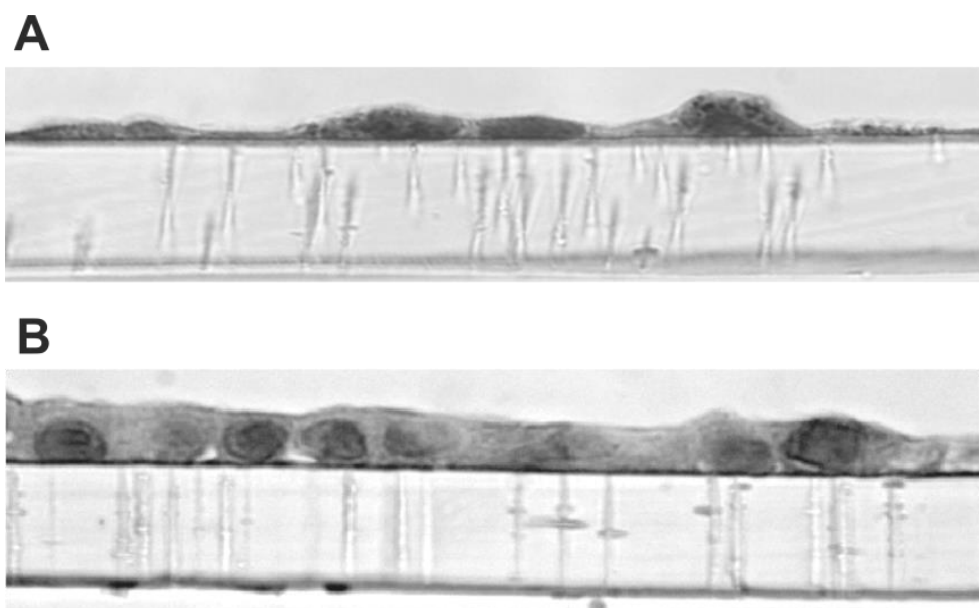
Figure II-13 Histological cross-sections of hAEpC and hAELVi
Histological cross-sections of hAEpC cells (A) and hAELVi.A cells (B) after seven days in culture on Transwell® filter under liquid-liquid condition (100x).

hAELVi.B cells cultivated under ALI conditions for seven days (Figure II-14A) showed no differences in the monolayer compared to those grown for 14 days under the same conditions (Figure II-14B). Also compared to hAELVi.A cells grown under LLC conditions (Figure II-13B), no differences could be observed.
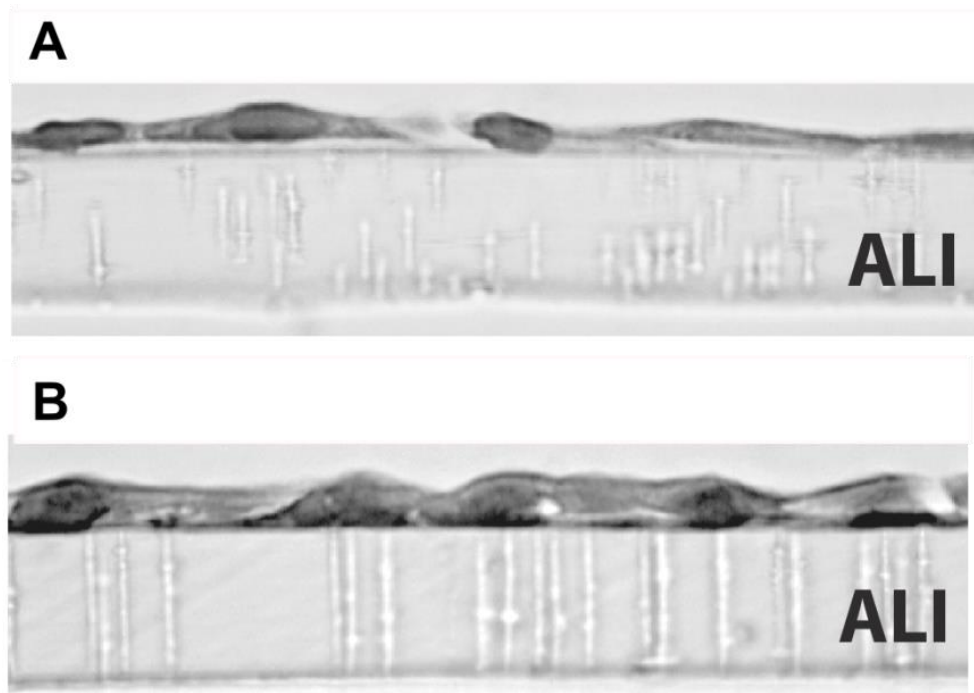
Figure II-14: Histological cross-section of hAELVi cells
Morphology of hAELVi.B grown under air-liquid interface (ALI) on Transwell® filter. Samples were fixed after seven days (A) or (B) 14 days. (A,B) Histological cross-sections (100X)

II.2.3.2 Confocal Laser Scanning Microscopy

II.2.3.2.1 Confirmation of epithelial identity with CD326

Via immunofluorescence the epithelial origin of hAELVi cells was verified. CD326 or EpCAM (for Epithelial Cell Adhesion Molecule) is a glycoprotein of ~40 kd with an expression pattern that is restricted to normal epithelial cells (Trzpis et al., 2007) and is used in the hAEpC isolation protocol to positively select the alveolar epithelial cells, mainly type II cells (Daum et al., 2012). Figure II-15 shows hAEpC cells (A) and hAELVi cells immunolabeled with anti-CD326 antibodies (green). Both cell models were growing for 8 days under LLC conditions. The CD326 is located in the cell membrane were it is involved in processes such as cell adhesion, signaling, cell migration, proliferation, and differentiation (Trzpis et al., 2007).
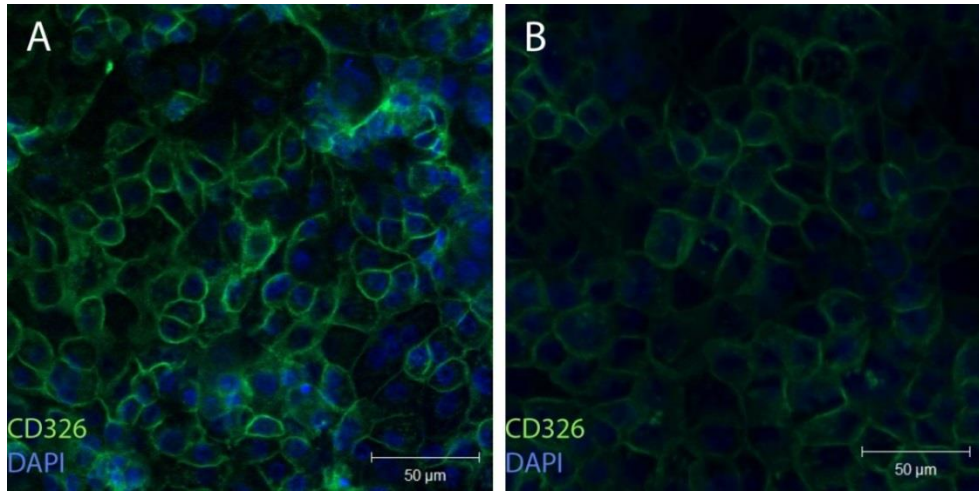
Figure II-15: Verification of epithelial origin.
Images from confocal laser scanning microscopy of hAEpC cells (A) and hAELVi cells (B), passage 18, growing under liquid-liquid condition (LLC) for 8 days, immunolabeled with anti-CD326 antibodies (green). Nuclei stained with DAPI (bue).

II.2.3.2.2 Analysis of tight junction proteins

The tight junctional complex is a crucial structure in terms of epithelial barrier formation. The tight junction complexes seal up the cell-cell contacts and hence restrict the paracellular transport of substances across an epithelium. The tight junction is the most apical structure of the epithelial junctional complex forming semipermeable intercellular diffusion barriers that control paracellular diffusion in a regulated manner (Matter and Balda, 1998). The here used immunolabeled antibodies are against the well-known tight junction proteins occludin and ZO-1 (Balda and Matter, 2000) to visualize the tight junctional complex. Occludin, a 60-65 kDA membrane-spanning protein that is widely expressed by essentially all epithelial and endothelial tissues, was the first transmembrane protein of tight junctions that was identified (Furuse et al., 1993). Zona occludens 1 (ZO-1) is a cytosolic plaque protein of 200-225 kDa (Anderson et al., 1988) which directly binds to occludin and is therefore associated with the tight junctional complex. It is supposed to link occludin to the actin cytoskeleton (Fanning et al., 1998).

Figure II-16 shows the immunolabeled tight junction proteins ZO-1 and occludin in hAELVi cells (A,B) and hAEpC cells (B,D), respectively. Both cell types were cultured under LLC (A,B) or ALI (C,D) conditions to directly compare the tight junction formation for both cases. The confocal laser scanning microscopy images do not reveal visual differences in the appearance of the examined tight junction proteins, in none of the cases. However, the cell borders of hAEpC cells appear more rigged than the cell-cell contacts of hAELVi cells. The cell size is variable in those two cell types; they feature smaller and bigger cells. An observation, which is typical

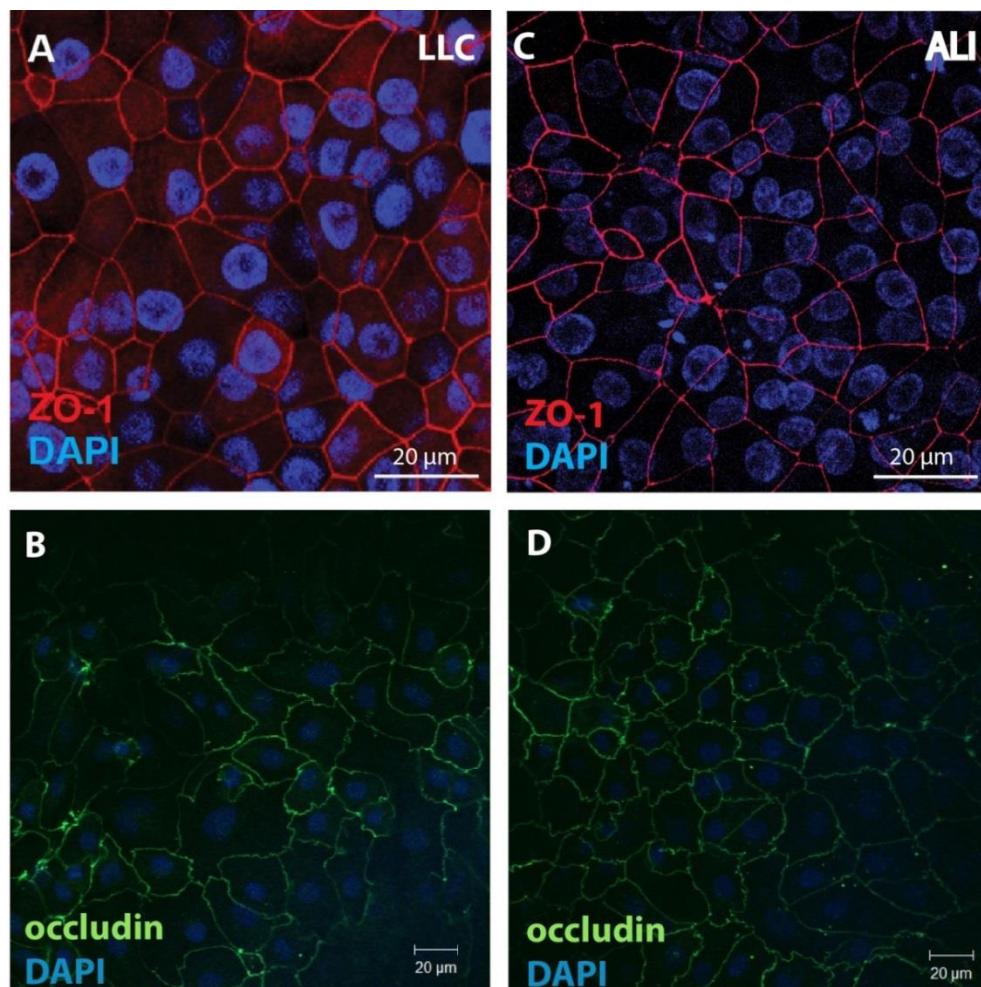for hAEpC cells, since these are a mixture of ATII cells differentiating into ATI-like cells.

Figure II-16: Immunofluorescence of tight junction proteins in hAELVi.B and primary cells under different culture conditions.
Images from confocal laser scanning microscopy of hAELVi.B (A,C) and hAEpC (B,D) growing under LLC (A,B) and ALI (C,D) conditions for 14 days (hAELVi) or 8 days (hAEpC), immunolabeled with anti-ZO-1 (red) antibody (A,C; hAELVi) or anti-occludin (green) antibody (B,D; hAEpC). Nuclei stained with DAPI (blue).

There was also no visual difference noticeable between the two hAELVi cell lines A and B, cultured on Transwell® filters or on cell culture plates regarding the formation of the tight junction protein occludin, as Figure II-17 demonstrates. The culture on Transwell® filters seems to facilitate the abovementioned variability in cell size.
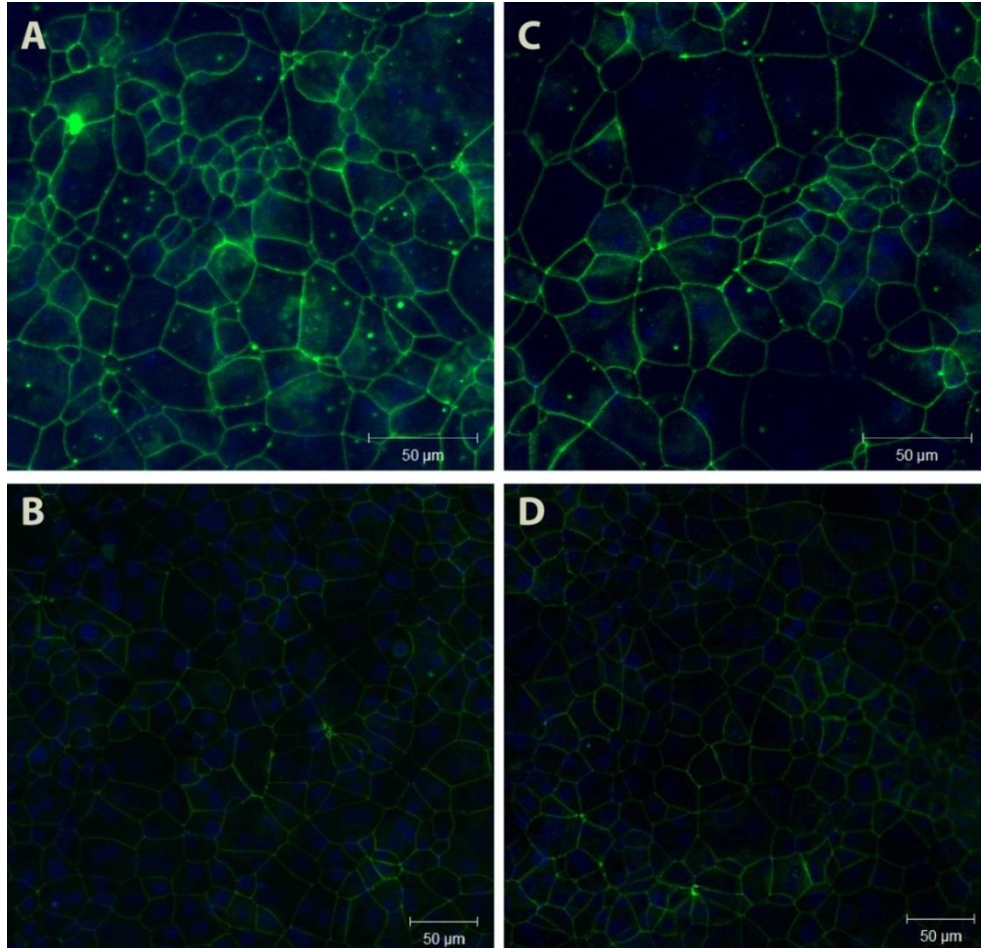
Figure II-17: Immunofluorescence of occludin in hAELVi.A and hAELVi.B
Images from confocal laser scanning microscopy of hAELVi.A (A,B) and hAELVi.B (C,D) growing on Transwell® filter (A,C) and cell culture chamber slides (B,D) for 14 days, immunolabeled with anti-occludin antibody (green). Nuclei stained with DAPI (blue).

II.2.3.3 Analysis of cellular ultrastructure using electron microscopy

To gain further insight and to confirm the CLSM results (Figure II-16 and Figure II-17) the cellular ultrastructure of hAELVi cells, again cultured under LLC and ALI conditions, was investigated with scanning and transmission electron microscopy.

II.2.3.3.1 Scanning electron microscopy

SEM images show the monolayer with clear cell-cell contacts, like seams, visible in Figure II-18. The cells, which were grown on Transwell® filters for 12 days, under LLC (A) or ALI (B) conditions, respectively, revealed no visible differences.
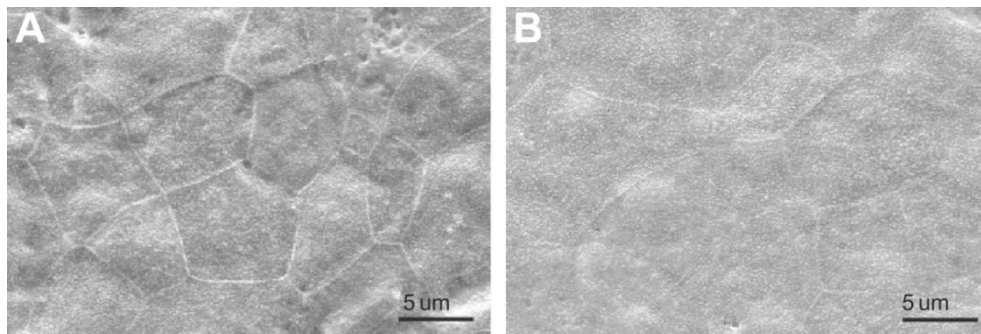
Figure II-18: SEM analysis of hAELVi cells.
Scanning electron microscopy of hAELVi.B on Transwells® after 12 days cultured under liquid-liquid (A) and air-liquid interface (B) conditions.

II.2.3.3.2 Transmission electron microscopy

Figure II-19 demonstrates the TEM pictures taken of hAELVi cells cultured under LLC (A,C) and ALI (B,D) conditions. Inter-digitations between the cells, sealed with tight junction complexes and desmosomes (A,B and C) are clearly visible as well as another typical ATI cell structure: caveolae. Caveolae are flask-shaped invaginations of the cell membrane, which pinch off to form discrete vesicles within the cell cytoplasm (Newman et al., 1999). The caveolae are located close to the apical cell membrane (C and D). These results, together with the observations regarding the tight junction complexes and TEER values corroborate the ATI-like character of the new cell line hAELVi.
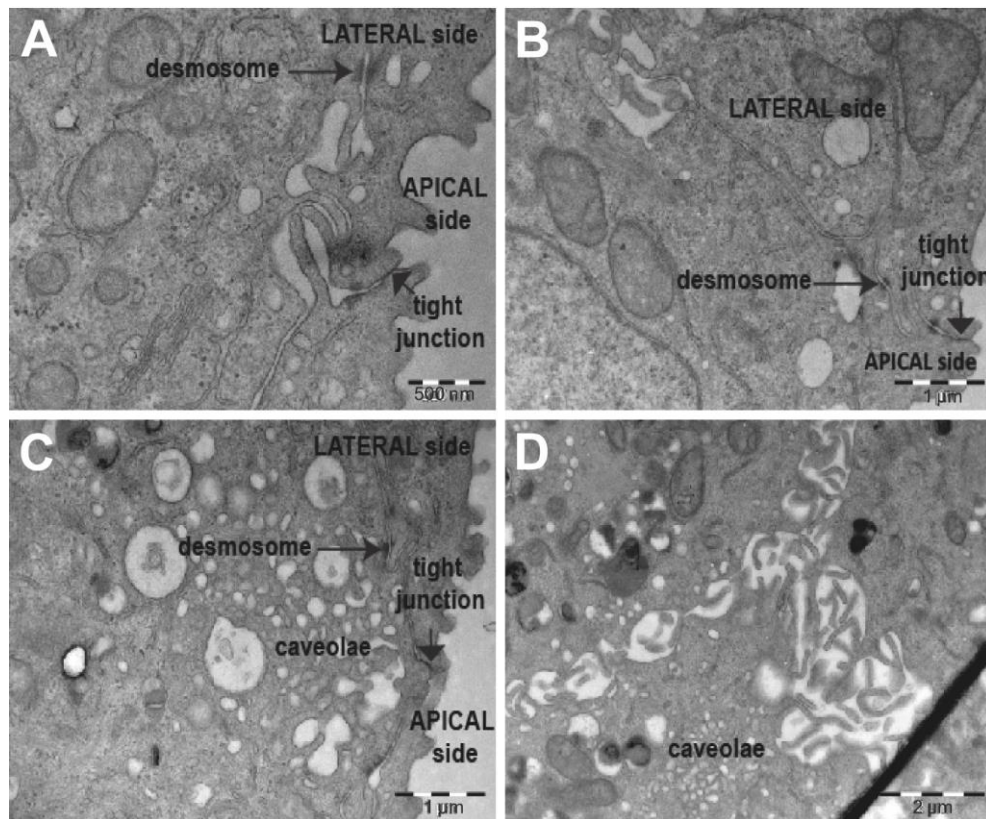
Figure II-19: Ultrastructure of hAELVi cells.
Transmission electron microscopy of hAELVi.B on Transwell® filters after 12 days, cultured under liquid-liquid culture (A,C) or air-liquid interface (B,D) conditions. Desmosomes (arrow), tight junctions (arrowhead) and caveolae are indicated in the TEM images.

II.2.4 rtPCR of lung-specific markers

Real-time PCR (rtPCR) showed the expression of alveolar epithelial cell-specific markers in hAELVi cells, compared to freshly isolated ATII cells, the precursor cells differentiating into the hAEpC model (Figure II-20). The markers caveolin (CAV-1), surfactant protein C (SP-C) and aquaporin 5 (AQP-5) were chosen, based on their known cell type-specific expression. Aquaporins are a family of water channels, of which AQP-5 is exclusively located on apical membranes of cells in the lacrimal gland and the salivary gland and in the lung, on apical membranes of type I epithelial cells (Nielsen et al., 1997; Funaki et al., 1998). SP-C is an ATII cell-specific marker, only expressed in this cell type (Phelps and Floros, 1991; Kalina et al., 1992) which, besides many other functions synthesize, secrete, and recycle all components of the surfactant proteins that regulates alveolar surface tension in mammalian lungs (Fehrenbach, 2001). CAV-1 is a 21–24 kDa integral membrane protein, which is the principal component of filaments that are crucial in the formation of caveolae (see Figure II-19C and D and (Rothberg et al., 1992; Newman et al., 1999)) Gil (Gil, 1983) estimated that 70% of the surface area of the ATI cell membrane is located within caveolae. We compared the expression level of these three proteins relative to the housekeeping gene GAPDH (Figure II-20); the results are shown as a percentage of their expression levels relative to freshly isolated human ATII cells. The expression of CAV-1 for both hAELVi cell lines was at a similar level as for primary culture type I like hAEpC (Figure II-20A). The type II cell marker SP-C however, could not be detected in either hAELVi cell line and was only marginally expressed in hAEpC (Figure II-20B). Conversely, AQP-5 was expressed at a low level in primary hAEpC, but could not be detected in the immortalized hAELVi cells (Figure II-20C).
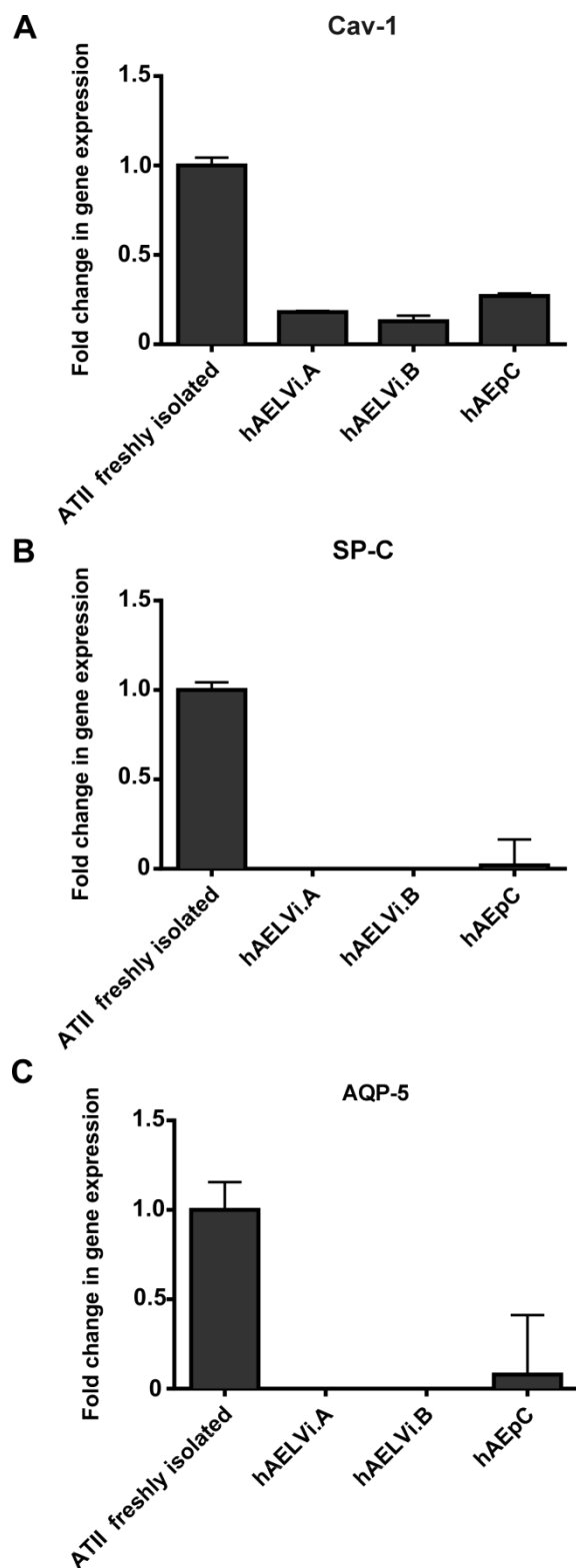
Figure II-20: rtPCR of lung markers.
(A) caveolin-1 (CAV-1), (B) surfactant protein C (SP-C), and (C) aquaporin-5 (AQP-5). The gene expression is shown as fold change in gene expression relative to the gene expression in freshly isolated ATII cells, whose expression was set 1.

II.2.5 Transport studies

The potential use of hAELVi cells as a model to predict drug absorption kinetics was also evaluated by measuring the apparent permeability coefficient (P_{app}) of the hydrophilic molecule sodium fluorescein (FluNa), typically used as a paracellular transport maker. The measurements were carried out by me (Figure II-21) and Stephanie Kletting (Figure II-22). Higher TEER is always accompanied with lower paracellular transport, and this relationship could be observed in hAELVi cells of lower passage number (p29) at day seven of culture on Transwell® filters under LLC conditions (Figure II-21). TEER of hAELVi.A was with 1200 Ω*cm^2 about 300 Ω*cm^2 lower than TEER of hAELVi.B and thus, as expected, the P_{app} of hAELVi.A was higher than the P_{app} of hAELVi.B, with $4.6 \cdot 10^{-7}$ cm/s and $3.0 \cdot 10^{-7}$ cm/s, respectively.
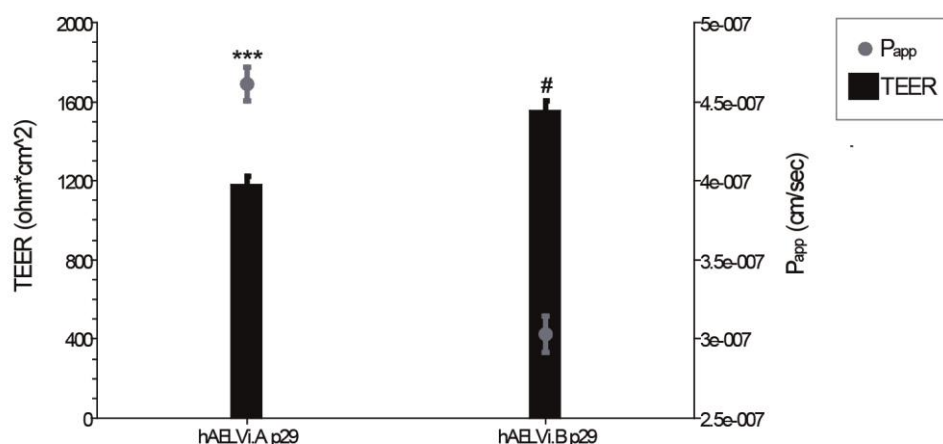
Figure II-21: Permeability assay in hAELVi cells (passage 29).
Transport of sodium fluorescein (FluNa) across monolayers of hAELVi.A and hAELVi.B after seven days, cultivated under LCC. The graph shows the relation of TEER and P_{app}. Data shown are mean ± SEM (n=2); ***P<0.001 Papp hAELVi.A *vs.* hAELVi.B; #P<0.05 TEER hAELVi.A *vs.* hAELVi.B

At a later time point the experiment was repeated with hAELVi.A cells of higher passage numbers, under LLC and ALI culture conditions, at two different time points (7 days and 14 days) and in the presence or absence of EDTA as a modulator of the tight junctional complex (Hochman and Artursson, 1994; Nagy et al., 1985). The results are shown in Figure II-22. Here the negative correlation between TEER and P_{app} was also observed and even more prominently at day 14 (Figure II-22.B), compared to day 7 (Figure II-22.A), when the cells displayed TEER of more than 1000 Ω*cm^2. In the presence of EDTA, due to its ability to chelate Ca^{2+} ions, which leads to a loosening of the tight junctions, the TEER dropped to almost zero and the P_{app} value of FluNa reached essentially the same maximal level, indicating complete

opening of the tight junctions under such condition, with more FluNa transported to the basolateral compartment. As mentioned above (see Figure II-9.C) the hAELVi cells exhibit higher TEER under ALI culture conditions compared to LLC culture conditions and hence lower P_{app} values, which is again confirmed in Figure II-22.
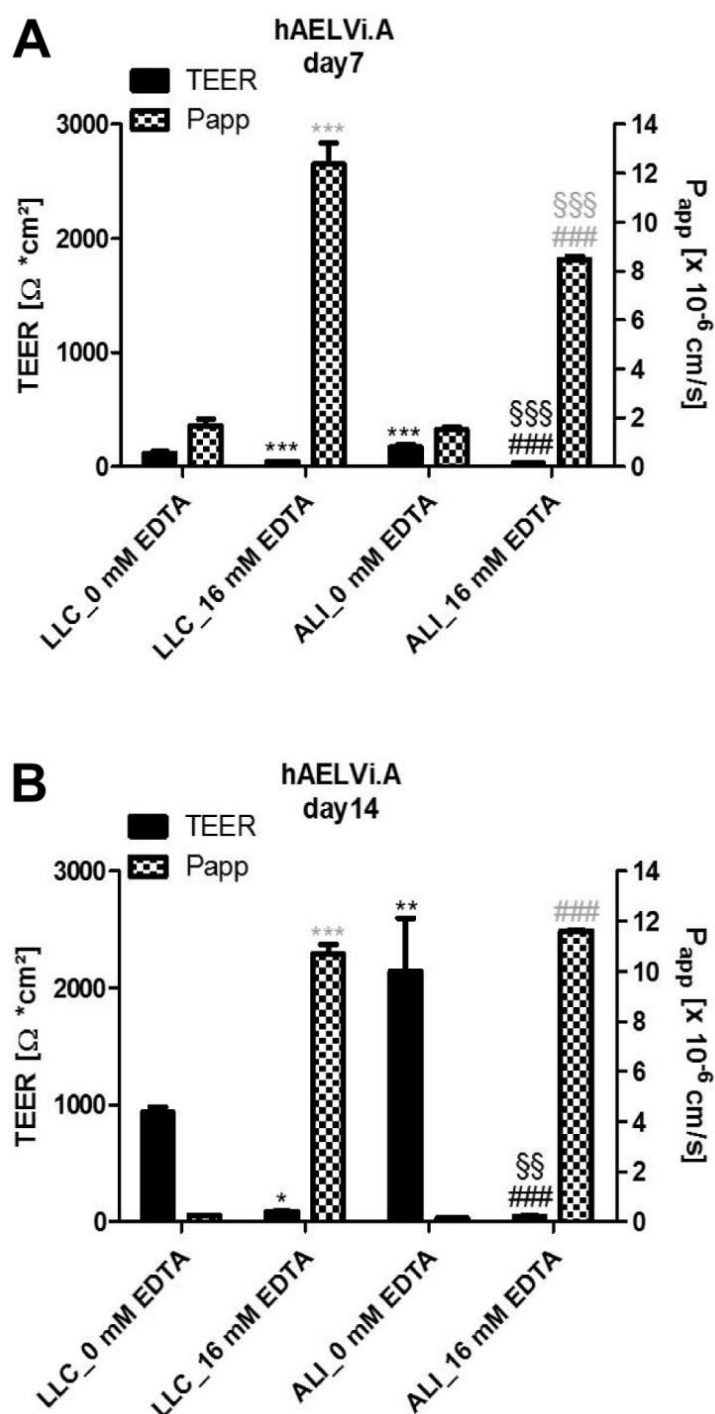
Figure II-22: Permeability assay in hAELVi cells

Transport of sodium fluorescein (FluNa) across a monolayer of hAELVi.A after seven days (A) or (B) 14 days, cultivated under LCC and ALI, respectively, and in the presence or absence of EDTA as a modulator of the tight junction complex. Both graphs show the relation of TEER and P_{app}. Data shown are mean $\pm$ SEM (n=3); *$P<0.05$; **$P<0.01$; ***$P<0.001$ *vs.* LLC_0 mM EDTA; ###$P<0.001$ *vs.* ALI_0mM EDTA; §§$P<0.01$; §§§$P<0.001$ *vs.* LLC_16 mM EDTA.

II.2.6 Data generated from other transfected cell populations

As shown in paragraph II.2.1.1 in total 51 infections were carried out. All infected cell populations were observed for their phenotype and performance in culture. Some of the cell populations did not survive as many passages as others (see Table II-4, Table II-5, and Table II-6) or didn't show interesting phenotypes, for example exhibited fibroblast-like shapes. Others were considered more interesting for further investigation. In the following paragraph, some of the data generated with other cell populations, that did not led to the new hAELVi cell line, is shown. Those cell populations were not discarded, but cryopreserved for possible future examination.

II.2.6.1 The TEER of different transfected polyclonal cell populations

In order to find a transfected cell pool, which is still able to develop TEER, different transfected cell populations were seeded on Transwell® filter devices with 0.4 μm pore size and examined over 15 to 21 days, in some cases in the absence or presence of doxycycline, depending on the transfection strategy (see Figure I-2) The cell populations for TEER measurement has been selected for their morphological resemblance of hAEpC in light microscopy images (see Figure II-25) and their growth behavior (e.g. no multilayer formation).

II.2.6.1.1 TEER of cell pools "8cGb" and "8cGe"

Two cell populations from isolation "hips62" with a set of eight constitutively expressed transformation genes (core, Nanog, ID1, ID3, E6, E7, EZH2 and Lmo-2, see Table II–3), "8cGb" and "8cGe", were seeded on Transwell® filters and TEER was measured over a time span of 21 days. TEER values were slightly higher than the filter without cells with values between 12 and 38 Ω*cm^2, which is negligible, showing almost no barrier formation (see Figure II-23)

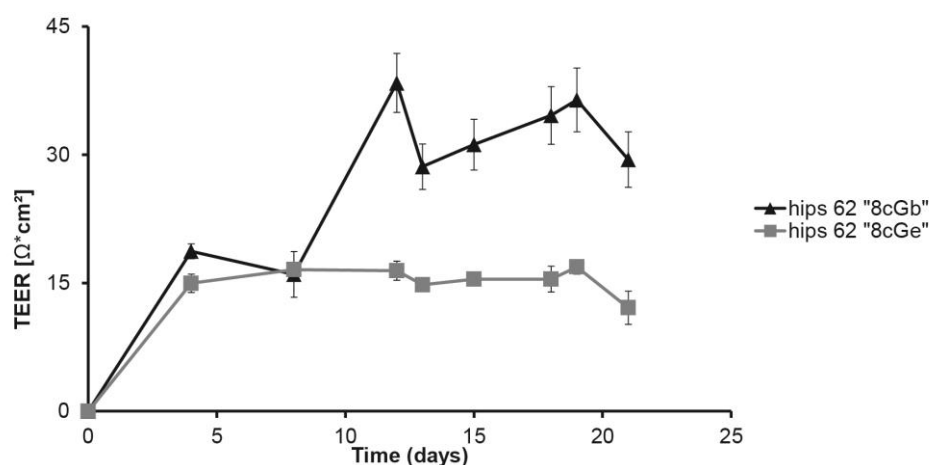**Figure II-23: TEER of cell pools "8cGb" and "8cGe".**
Isolation "hips62" was transfected with a set of 8 constitutively expressed transformation genes and TEER was measured in passage 12 over 21 days. Data shown is mean ±SEM.

II.2.6.1.2 TEER of cell pools "JSARLTT2", "JSCMVTA2 ID1/ID3/E6", and "JSARTA3 ID1/ID3/E6"

The three transfected cell populations "JSARLTT2", "JSCMVTA2 ID1/ID3/E6", and "JSARTA3 ID1/ID3/E6" were cultured on Transwell® filters in passage 5 and TEER was measured over a time span of 13 days as shown in Figure II-24. The cells were either cultured in the absence (-DOX) or presence (+DOX) of doxycycline, which is the molecule that, together with the TA protein, controls the tet-dependent promoters of the three transformation genes ID1, ID3 and E6 in the here used constructs. The TEER of "JSARLTT2" was significantly higher on all measured time points in the presence of doxycycline, but nevertheless still negligibly low, with values not higher than 24 Ω*cm², so that in neither case a barrier formation took place. "JSCMVTA2 ID1/ID3/E6" supplemented with doxycycline showed a significant higher TEER in comparison to doxycycline absence on day 13 of culture, but, as in the case of"JSARLTT2", the TEER is with 16 Ω*cm² negligible. Also "JSARTA3 ID1/ID3/E6" did not develop higher TEER values than 15 Ω*cm², and did not show significant differences regarding the presence or absence of doxycycline.
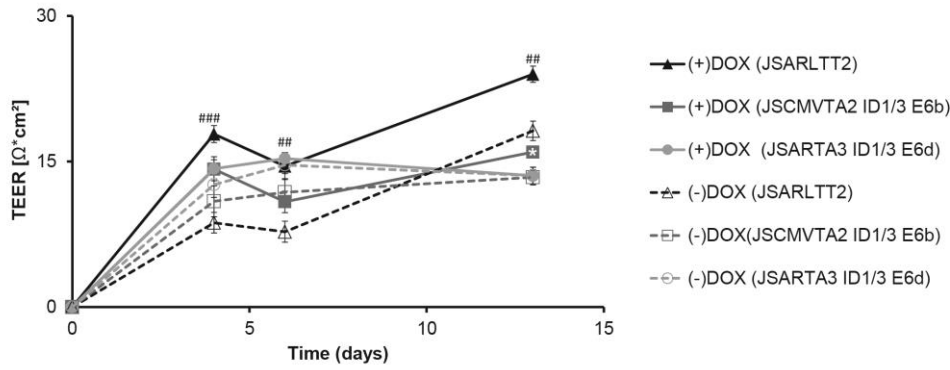
Figure II-24: TEER of cell pools "JSARLTT2", "JSCMVTA2 ID1/ID3/E6b", and "JSARTA3 ID1/ID3/E6d"

Isolation "hips62" was transfected with 3 transformation genes, namely ID1, ID3 and E6, or two transformation genes, namely Large T-Antigen (LT) and hTert (T), under the control of a tet-dependent promoter and a particular vector carrying the transactivator (TA) protein, which is either under the control of a constitutively expressed (JSCMVTA2) or auto-regulated (JSARTA3) promoter system. Cells in passage 5 were cultivated on Transwell® filter for 13 days and TEER was measured on days 3, 6 and 13. Data shown are mean ±SEM. *P<0.05 (+) DOX vs. (-)DOX "JSCMVTA2 ID1/ID3/E6". ##P<0.01 and ###P<0.001 (+)DOX vs. (-)DOX "JSARLTT2".

II.2.6.2 Morphology of several infected cell populations

The morphology of the three transfected cell populations "JSARLTT2" (Figure II-25A), "JSCMVTA2 ID1/ID3/E6b" (Figure II-25B), and "JSARTA3 ID1/ID3/E6d" (Figure II-25C), whose TEER values (< 30 Ω*cm^2) are shown in Figure II-24, differs visibly in passage 5. The light microscopic image was taken when the cells reached confluence. "JSARLTT2" and "JSARTA3 ID1/ID3/E6d" show wide and flat cell morphology and form monolayers, while "JSCMVTA2 ID1/ID3/E6b" exhibits a more fibroblast-like morphology with long, spindle-shaped cells that form multilayers.
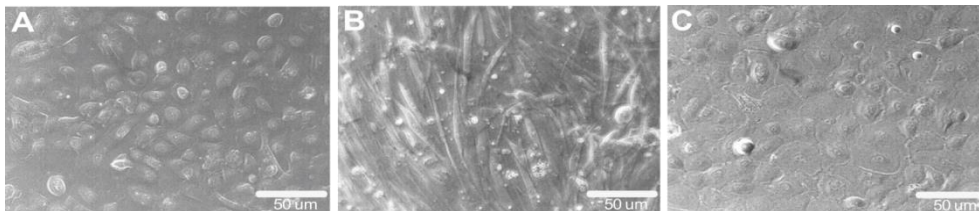

Figure II-25: Light microscopic image of 3 different transfected cell populations. "JSARLTT2" (A), "JSCMVTA2 ID1/ID3/E6b" (B), and "JSARTA3 ID1/ID3/E6d" (C) in passage 5, photographed when reached confluence. Magnification 100x.

III. DISCUSSION

Primary cells are the gold standard for many applications, but due to their limited availability from healthy human donors and their short, lifespan they are not easily accessible, and thus the use of immortal cell lines is in many cases preferred or inevitable. Especially in terms of primary human alveolar cells (hAEpC) the abovementioned problems apply and impede the use of these cells in large scaled experiments. Also the reproducibility of results obtained from hAEpC can be questionable due to the donors' genetic heterogeneity and anamnesis. Figure II-4 demonstrates that not all of the isolations of hAEpC cells could be used for experimentation and one should bear in mind that the isolation is a cost-intensive procedure. Prior to using the cells, their barrier integrity has to be measured, and if the barrier is impaired the cells cannot be used, at least for drug transport studies.

Carcinoma-derived pulmonary cell lines, e.g. the widely used A549 cells (Foster et al., 1998), and other cancer cell lines are beneficial for studying cancer development, but hardly represent normal epithelial cells e.g. a blastoma-derived cell line (Camerlingo et al., 2011) or an *in vitro* carcinogenesis model, where ATII cells are exposed to Tobacco-specific carcinogens (Mennecier et al., 2014). Spontaneous immortalization of human epithelial cells by overcoming senescence barriers is a known factor in carcinogenesis, and malignity often depends on which alterations led to immortality (Stampfer and Yaswen, 2003). Genetic instability leading to tumor development due to defects of cell cycle checkpoints and DNA mismatch repair (Damia and D'Incalci, 2010) and non-defined genetic alterations, chromosomal heterogeneity and aneuploidy of tumor cells (Castro-Gamero et al., 2013) are often observed in tumor-derived cell lines, too. Furthermore transformation can be linked to aberrant growth independent from anchorage. *In vitro* immortalization aims at achieving an unlimited lifespan without transformation, e.g. by insertion of specific genes that interfere with the cell cycle and apoptosis control. The resulting cell line should ideally show an unlimited lifespan, and contact-inhibited motility and proliferation. The new immortal alveolar cell line hAELVi complies with these criteria. The characterization of this new cell line was recently published (Kuehn et al., 2016)

Figure II-1 shows the sigmoidal growth curve of hAELVi cells, which confirms together with the analysis of light microscopic images of the cells (see Figure II-11 and Figure II-12) that they grow in contact-inhibited monolayers. Of course, this is not sufficient evidence to determine whether the hAELVi cells are immortalized or transformed. To answer this question it is necessary to examine the capability to proliferate anchorage independently *in vitro,* and *in vivo* by crafting the cells into immunosuppressed or -compromised mice and observe tumor formation (Lipps et al., 2013) To immortalize primary human alveolar cells different immortalization

strategies were used in this work (see Figure I-2). In all cases hAEpC cells were transfected with lentiviral vectors to insert genes that alter cell cycle and proliferation control. Nine cell populations with prolonged life span were generated; one resulted from the transfection with SV40 LTAg and humane telomerase (hTert) under the translational control of an autoregulated tet-dependent promoter ("JSARLTT2", see Table II-5 and Figure II-24). The use of a temperature-sensitive mutant of hTert and the catalytic subunit of LT was previously reported by Tetley *et al.* (van den Bogaard et al., 2009) to immortalize ATII cells, resulting in an ATI cell line, TT1, without barrier properties, suitable for inflammatory response studies (van den Bogaard et al., 2009) or nanoparticle uptake studies (Kemp et al., 2008). JSARLTT2 did not show the desired reaction, namely the differentiation from proliferating cells into functional differentiated ATI cells with TEER upon doxycycline withdrawal. The TEER measurements with and without doxycycline showed no significant difference. The cell line was cryopreserved and excluded from further studies. Two more cell populations with prolonged lifespan were generated using three different oncogenes, namely ID1, ID3 and E6, under the translational control of tet-dependent promoters: "JSCMVTA2+JStetID1/ID3/E6b" and "JSARTA3+JStetID1/ID3/E6d". Those genes were chosen based on previous results obtained by Dr. Nicole Schneider-Daum and Dr. Tobias May. The ID3 oncogene was later found to be integrated into the hAELVi cell genome (see Figure II-2) However, none of these three lines developed the desired barrier properties of hAEpC cells, neither with, nor without doxycycline treatment (May et al., 2004, 2007). This approach was chosen to counter the often occurring de-differentiation caused by immortalization. ATI-like cells are supposed to be "terminally differentiated" cells, so by dividing the proliferation and the differentiation this problem may be bypassed by acting like a switch (Gossen and Bujard, 1992; Gould et al., 2000). Those generated cell lines either immortalized spontaneously, which is not common in alveolar epithelial cells and hence unlikely, or the tet-dependent promoter system somehow failed to work in the desired manner and led to a tet-independent regulation.

Following another approach to reduce the possible de-differentiation of cells caused by transformation, the cells were transduced with a set of 33 genes, which, in the right combination, are able to immortalize various cells types (Klein, 2012). The new immortal hAELVi cell line was generated by infection of hAEpC isolation 63 with a mixture of 33 "mild" oncogenes (see Table II-6). It was shown, that for certain cell types the immortalization can be reproducible, if the right gene combination is found (Schwerk et al., 2013; Klein, 2012). The use of a mixture of 33 different genes increases the possibility to find a combination, by chance, that enables the cell to overcome senescence and enter proliferation. 7 of 33 genes were found integrated in hAELVi cells (see

Figure II-2), namely *Id2, Id3, E7, Bcl2, core, myc* and *Nanog.* Id2 enhances cell proliferation by binding to the tumor suppressor retinoblastoma protein pRb (Iavarone et al., 1993; Lasorella et al., 1996). Id2 interacts in certain tumors with myc (Cotta et al., 2008). Id3 acts in a similar manner as Id2; they play a role in tumorigenesis (DiVito et al., 2013; May et al., 2013). Id3 seems to be regulated by myc in differentiation processes (Light et al., 2005). The HPV protein E7 is a strong oncogene that targets the p53 and pRb pathways of cell cycle regulation and tumor suppression (Kiyono et al., 1998; Nevins, 1994). The hepatitis C virus core protein was used to immortalize primary human hepatocytes (Ray et al., 2000); it seems to inhibit p53 and upregulate myc in these cells (Basu et al., 2002). Nanog is uniquely expressed in embryonic stem cells and plays a role in the induction of pluripotent stem cells and the differentiation of those cells into certain cell types (Yamanaka et al., 2007; Van Haute et al., 2009). It would be interesting to infect hAEpC cells with this set of 7 genes aiming at reproducing the immortalization as it was shown by Schwerk *et al.* and in the work of Franziska Klein (Schwerk et al., 2013; Klein, 2012). Eventually, using a tet-dependent promoter system and the here found set of 7 genes would lead to a conditional immortalized alveolar cell line.

The here used strategy led to an immortalized cell line of human alveolar epithelial cells, hAELVi, exhibiting barrier properties comparable to those of primary ATI-like cells, e.g. high trans-epithelial electrical resistance. Previous approaches reported by others have led to the development of immortalized human lung cell lines, which are well suited for many applications, *e.g.* nanoparticle-uptake (Kemp et al., 2008), inflammatory response (van den Bogaard et al., 2009), or cancer pathogenesis (Camerlingo et al., 2011; Mennecier et al., 2014). However, these cells lack the capability to form functional tight junctions, which are needed to build a formidable diffusion barrier also to smaller hydrophilic molecules. Consequently, these cell lines are probably of limited value for conducting transport studies across the notoriously tight alveolar epithelium. The same is true for the frequently used human lung adenocarcinoma cell line A549 (Foster et al., 1998). Human lung cell lines, which do form tight junctions are available, such as Calu-3 (Grainger et al., 2006; Daum et al., 2009) and 16HBE14o- (Forbes, 2003); however, these are derived from the upper airways, and show columnar rather than squamous shape, and feature cilia as well as mucus. Due to lack of better alternatives, these cell lines have been used to assess pulmonary drug transport *in vitro*, either alone or in co-culture with other primary cells or cell lines (Hermanns et al., 2004; Lehmann et al., 2011). The relevance of such studies to predict transport across the alveolar epithelium, however, must be interpreted very cautiously.

However, the new cell line hAELVi is capable of building TEER values higher than 1500 $\Omega \cdot cm^2$, comparable to the TEER of ATI-like cells (see Figure II-6). The two cell populations that were isolated from the transfected cell pool slightly differ in

the time they need to reach TEER values over $1500\ \Omega \cdot cm^2$ – hAELVi.A is more delayed than hAELVi.B, but both hAELVi lines need more time to reach the desired value in comparison to ATI-like cells. This may seem a disadvantage due to higher costs generated by longer culturing and hence higher medium consumption, but actually the costs will be lower due to the elimination of the isolation procedure. But the huge advantage hAELVi cells show regarding the TEER is that they maintain the high TEER for several days up to weeks (see Figure II-6), where primary ATI-like cells normally hold their high TEER for a maximum of 4 days. This enables the implementation of hAELVi cells in long-time studies, either e.g. for pharmaceutical applications or infection research.

The observation of the TEER over a large span of passages showed that the TEER development of hAELVi stayed rather stable (see Figure II-7). From passage 18 to passage 75 the hAELVi cells did not lose their ability to form a tight barrier. Passage 75 was the oldest and latest passage measured, so far. In other epithelial cell models, such as the widely used Caco-2 cell line, a model of the intestinal epithelium, the TEER can differ highly depending on the passage number, showing physiological and ultra-structural changes (Lu et al., 1996). Of course, hAELVi cells have to be passaged further to investigate late passage-related alterations in TEER development or other properties. The maximum TEER value that was reached in the different passages increased from early to late passages (see Figure II-8), which was also observed in the above mentioned Caco-2 cells (Briske-Anderson et al., 1997). In general, the proliferation of cells always generates mutations that can alter the phenotype of cell lines, so that the use of early passage-batches is recommended and the frequent control of the cell batch is crucial. Figure II-8 also shows the loss of one of the originally three isolated cell lines from the transfected gene pool, hAELVi.C, due to the loss of the ability to develop TEER after passage number 20. The cell line was excluded from further studies.

The fact that hAELVi cells can be cultured under LLC or ALI conditions offers the possibility to use the cell line not only to investigate e.g. the transport of soluble components and in general liquid formulations but also aerosols or dry formulations. The administration of drugs via the pulmonary route allows local or systemic effects. Several set ups has been used to study the deposition of e.g. aerosols from dry powder inhalers (PADDOCC - Pharmaceutical Aerosol Deposition Device on Cell Cultures, (Hein et al., 2011)) or aerosolized nanoparticles in suspension (ALICE - (Brandenberger et al., 2010)). hAELVi cells could be implemented in these devices and exposed to aerosols and particles, not only for drug delivery studies but also for the toxicity assessment of air-borne particles of many different materials. In comparison with hAEpC cells the hAELVi cells tend to increase their TEER upon ALI culture conditions, while the hAEpC cells tend to decrease their TEER compared to LLC conditions (see Figure II-9). hAELVi cells form an even tighter

barrier when cultured in the more physiological relevant manner. Transport studies with the hydrophilic molecule sodium fluorescein (FluNa) typically used as a paracellular transport maker confirmed the tight barrier of hAELVi cells. A next important step must be the examination of active transporters of peptides, e.g. PEPT-2 (Groneberg et al., 2001), or organic cations OCT (Salomon and Ehrhardt, 2012) as well as efflux systems, such as MDR1/P-gp (Cordon-Cardo et al., 1990) or BCRP (Ejendal and Hrycyna, 2002), in further experiments to enable the comparison with the primary cells, and other cell lines to assess the applicability of hAELVi cells for above-mentioned studies.

The morphology of hAELVi cells does not resemble the squamous morphology of ATI-like cells (see Figure II-13), but rather the cuboidal shape of ATII cells or the A549 cells, too. Nevertheless, hAELVi cells form growth-inhibited monolayers and, as demonstrated by (ultra)structural and functional studies, form tight intercellular junctions. Transmission electron microscopy (see Figure II-19) showed clearly the tight junctional complexes sealing the paracellular space between adjacent cells. Also desmosomes are visible, which are, as well as tight junctions, cell-cell contacts, but are mainly responsible for intercellular adhesion to resist forces of mechanical stress in epithelia and for cell-substrate contacts (Green and Jones, 1996). Interdigitations, downright interlocking the cell membranes, were also observed and promote as well as desmosomes the intercellular attachment and stability. Tight junctions, however, are responsible for the tightening of the epithelium and the regulation of the passage of water, ions and neutral molecules via the paracellular pathway (Godfrey, 1997). Tight junctions are located at the apicolateral borders of the cells. In the here shown immunofluorescence imaging of the tight junction components occludin and zonula occludens 1 (see Figure II-16 and Figure II-17) this location was confirmed in hAELVi cells. The immune-staining shows the borders of the cells clearly and regularly. Transmission electron microscopy images show that the cell borders are even visible on the apical surface of the monolayer looking like seams. Since it is known that the alteration of tight junction integrity may be important for the course of infections, asthma and cystic fibrosis (Vermeer et al., 2009; Godfrey, 1997), hAELVi cells may also help to understand the role of tight junctions in disease development.

The ultrastructural analysis demonstrated also the presence of caveolae at the plasma membrane. Caveolae are flask-shaped invaginations of the cell membrane, which pinch off to form discrete vesicles within the cell cytoplasm (Newman et al., 1999). CAV-1 is a protein of the caveolae membrane system that plays a role in the signaling platform and in the transport of macromolecules through the cell (Gumbleton, 2001); its expression increases during the transition from the ATII phenotype to the ATI phenotype (Fuchs et al., 2003) and thus, is commonly used as an ATI marker. To compare the expression of CAV-1 in hAELVi cells, in freshly

isolated ATII cells and ATI-like cells, rtPCR was performed. The expression of CAV-1 in hAELVi cells resembled that in ATI-like cells, but for both cell types the expression was lower than in ATII cells. Although CAV-1 expression should increase during ATI differentiation, Fuchs et al. also showed that the expression in freshly isolated ATII cells is almost quite as high as in terminally differentiated ATI-like cells cultured for 8 days. Only hAEpC cells cultured for 3 or 5 days, and considered yet not terminally differentiated, showed very low CAV-1 expression (Fuchs et al., 2003). The relatively high expression of CAV-1 in freshly isolated ATII cells, which was also observed here, even in a more extreme way, might be due to contaminating subpopulations of cells, such as endothelial cells or fibroblasts, within the freshly isolated ATII cells (Fuchs et al., 2003), or more likely ATI cells, which survived the isolation procedure, but will not survive the further culturing procedure to achieve hAEpC cells.

A typical ATII cell-related structure, the lamellar bodies, was not observed in the morphological and ultrastructural studies. Lamellar bodies are unique organelles, exclusively occurring in ATII cells, that are responsible for the production, storage, secretion and recycling of most of the alveolar surfactant components, which are mainly phospholipids and proteins (Fehrenbach, 2001; Schmitz and Müller, 1991). Also A549 cells, which strongly resemble the ATII-phenotype have lamellar bodies and show secretion of phospholipids (Shapiro et al., 1978). The surfactant protein C, SP-C is a common ATII cell marker. As was expected due to the absence of lamellar bodies in hAELVi cells, no SP- transcripts were detectable via rtPCR. In comparison, in freshly isolated ATII cells SP-C transcripts were detected, as well as in a very small amount in ATI-like hAEpC cells. This could be due to not yet complete differentiation of the originally isolated ATII cells into the ATI phenotype. The presence of caveolae and CAV-1 transcripts together with the absence of multilamellar bodies and SP-C transcripts, indicate that the new immortal hAELVi cell lines resemble an ATI-like rather than an ATII-like phenotype.

Another often used ATI marker is AQP-5, a water channel protein expressed in the apical side of ATI and bronchial epithelium cells (Nielsen et al., 1997; McElroy and Kasper, 2004) and seems to regulate the volume of the ATI cell (King and Agre, 1996). AQP-5 transcripts could not be detected in the immortalized hAELVi cell lines. The reasons for this result and its implication for epithelial transport studies deserve further investigation like immunofluorescence studies, because the marker has been found in cells using labeled antibodies, even though it could not be detected at the transcriptional level (Hermanns et al., 2009). In ATI-like hAEpC cells AQP-5 was found to be expressed, as expected. Worth mentioning, once again, as it was observed with CAV-1, the highest expression of AQP-5 was found in freshly isolated ATII cells. These cells seem to be contaminated with other cell types, probably ATI cells,

which survived the isolation procedure, but will not survive the further culturing procedure to achieve hAEpC cells.

Other lung cell type-specific markers should be investigated to further characterize hAELVi cells, e.g. the receptor for advanced glycation endproducts (RAGE). This is an interesting marker, which could provide more information about the differentiation status of hAELVi cells. RAGE was shown to be expressed upon the trans-differentiation of ATII into ATI-like cells *in vitro* (Buckley and Ehrhardt, 2010) and to promote the spreading of said cells contributing to achieve their squamous phenotype (Demling et al., 2006).

To model the air-blood barrier various advanced co-culture systems are used that are comprised of more than one cell type. Some of these models use primary cells, e.g. in a triple co-culture model using hAEpCs, monocyte-derived macrophages (MDMs) and monocyte-derived dendritic cells (MDDCs) from human blood (Lehmann et al., 2011). Lehman et al. show that the use of primary ATI-like cells due to their barrier properties should be preferred to cell lines, such as A549 or 16HBE14o-, for this triple co-culture system, even though the effort and costs are higher. Blank et al. use the above-mentioned triple co-culture with 16HBE14o-, MDMs and MDDCs as a model of the airway wall to study the cellular interaction of MDMs and MDDCs, in this case particle exchange, when exposed to polystyrene micro particles (Blank et al., 2011). Maybe hAELVi cells could offer an alternative to hAEpCs or 16HBE14o-, respectively, in these co-culture models. Also other co-culture models use A549 cells or 16HBE14o- cells as the cell model for the alveolar epithelium, and could profit from the exchange of those cell lines, which are not well suited to mimic ATI cells, for the new hAELVi cell lines, e.g. a model with A549 and peripheral blood mononuclear cells to investigate interleukin and interferon responses (Torvinen et al., 2007). Besides the study of immune or inflammation responses, co-cultures with A549 cells are also used to mimic the actual alveo-capillary barrier, e.g. with A549 cells in combination with primary human microvascular endothelial cells (Hermanns et al., 2004; Kasper et al., 2011). In this case it is even more important that the crucial barrier properties provided by ATI cells are reflected by the employed cell types, which is not the case for A549. Future studies could show the benefit from hAELVi cells for alveo-capillary models of the air-blood barrier.

Recently, the generation of lung and airway epithelial cells from human pluripotent stem cells (hPSCs) was reported by Huang et al. using a protocol that achieves high yields of progenitor cells committed to a lung fate. They showed the differentiation into functional lung and airway cells *in vivo* and *in vitro* (Huang et al., 2014). This is, without question a great achievement and offers a new possibility to obtain alveolar epithelial cells without the need for donated tissue from lung resection surgeries, which is always limited. Generation of alveolar cells from hPSCs can overcome this shortage, as well as alveolar cell lines can. The big advantage cell lines

have compared to hPSC-generated lung cells is their easy handling. hAELVi cells are easy to cultivate; they need just one (commercially available) cell culture medium and they are easy to store by common cryo-preservation techniques. The isolation of hAEpCs from human donor tissue and also the generation of alveolar cells from hSPCs are highly time- and money-consuming tasks and need more advanced techniques than the use of an immortal cell line. hAELVi cells, in contrast, could be used by groups that do not have the resources, tools and expertise required for the before-mentioned cell models.

IV. Conclusion

In summary, the new cell line hAELVi displays morphological as well as physiological similarities with ATI cells. Most importantly, these cells develop tight intercellular junctions and high TEER ($>$ 1000 Ω^*cm^2) resulting in a formidable diffusion barrier to a hydrophilic marker molecule. hAELVi cells show great potential to become a model for the alveolar epithelium or even for the air-blood barrier if combined with other relevant cell types, e. g. with immune cells or epithelial cells. As a model for the alveolar epithelium, as monoculture or utilized in advanced co-cultures, hAELVi cells could be an alternative to animal testing, both in the context of pulmonary drug delivery as well as inhalation toxicology and help to implement the 3R principle (Replacement, Refinement, Reduction). Besides serving as a model of the air-blood barrier for drug transport studies, metabolism studies and toxicity assessments, hAELVi cells may also help to understand the role of tight junctions in disease development, e.g. infections, asthma and cystic fibrosis, since it is till date the only immortal alveolar cell line exhibiting functional tight junctions. hAELVi cells could be an alternative to A549 cells in advanced co-culture systems, providing the crucial barrier properties those cells are lacking and thus help to improve the reflection of the *in vivo* situation. The comfortable handling of the hAELVi cell line, its low maintenance costs, compared to primary cells or hPSC-derived lung cells, and of course its unlimited availability makes it an ideal tool for large-scaled experiments, offering a high reproducibility of results for a broader group of scientists.

References

Anderson, J., B. Stevenson, L. Jesaitis, D. Goodenough, and M. Mooseker. 1988. Characterization of ZO-1, a protein component of the tight junction from mouse liver and Madin-Darby canine kidney cells. *J. Cell Biol.* 106:1141–1149. doi:10.1083/jcb.106.4.1141.

Andreeva, A. V, M.A. Kutuzov, and T.A. Voyno-Yasenetskaya. 2007. Regulation of surfactant secretion in alveolar type II cells. *Am. J. Physiol. Lung Cell. Mol. Physiol.* 293:L259–71. doi:10.1152/ajplung.00112.2007.

Balda, M.S., and K. Matter. 2000. Transmembrane proteins of tight junctions. *Semin. Cell Dev. Biol.* 11:281–9. doi:10.1006/scdb.2000.0177.

Barkauskas, C.E., M.J. Cronce, C.R. Rackley, E.J. Bowie, D.R. Keene, B.R. Stripp, S.H. Randell, P.W. Noble, and B.L.M. Hogan. 2013. Type 2 alveolar cells are stem cells in adult lung. *J. Clin. Invest.* 123:3025–36. doi:10.1172/JCI68782.

Basu, A., K. Meyer, R.B. Ray, and R. Ray. 2002. Hepatitis C Virus Core Protein Is Necessary for the Maintenance of Immortalized Human Hepatocytes. *Virology.* 298:53–62. doi:10.1006/viro.2002.1460.

Blank, F., M. Wehrli, A. Lehmann, O. Baum, P. Gehr, C. von Garnier, and B.M. Rothen-Rutishauser. 2011. Macrophages and dendritic cells express tight junction proteins and exchange particles in an in vitro model of the human airway wall. *Immunobiology.* 216:86–95. doi:10.1016/j.imbio.2010.02.006.

van den Bogaard, E.H.J., L.A. Dailey, A.J. Thorley, T.D. Tetley, and B. Forbes. 2009. Inflammatory response and barrier properties of a new alveolar type 1-like cell line (TT1). *Pharm. Res.* 26:1172–80. doi:10.1007/s11095-009-9838-x.

Bosquillon, C. 2010. Drug Transporters in the Lung — Do They Play a Role in the Biopharmaceutics of Inhaled Drugs ? 99:2240–2255. doi:10.1002/jps.

Brandenberger, C., B. Rothen-Rutishauser, C. Mühlfeld, O. Schmid, G.A. Ferron, K.L. Maier, P. Gehr, and A.-G. Lenz. 2010. Effects and uptake of gold nanoparticles deposited at the air-liquid interface of a human epithelial airway model. *Toxicol. Appl. Pharmacol.* 242:56–65. doi:10.1016/j.taap.2009.09.014.

Bray, B.A. 2001. The role of hyaluronan in the pulmonary alveolus. *J. Theor. Biol.* 210:121–30. doi:10.1006/jtbi.2001.2305.

Briske-Anderson, M.J., J.W. Finley, and S.M. Newman. 1997. The influence of culture time and passage number on the morphological and physiological development of Caco-2 cells. *Proc. Soc. Exp. Biol. Med.* 21:248–257. doi:10.3181/00379727-214-44093.

Buckley, S.T., and C. Ehrhardt. 2010. The receptor for advanced glycation end products (RAGE) and the lung. *J. Biomed. Biotechnol.* 2010:917108.

doi:10.1155/2010/917108.

Bur, M., H. Huwer, C.-M. Lehr, N. Hagen, M. Guldbrandt, K.-J. Kim, and C. Ehrhardt. 2006. Assessment of transport rates of proteins and peptides across primary human alveolar epithelial cell monolayers. *Eur. J. Pharm. Sci.* 28:196–203. doi:10.1016/j.ejps.2006.02.002.

Bur, M., B. Rothen-Rutishauser, H. Huwer, and C.-M. Lehr. 2009. A novel cell compatible impingement system to study in vitro drug absorption from dry powder aerosol formulations. *Eur. J. Pharm. Biopharm.* 72:350–357. doi:10.1016/j.ejpb.2008.07.019.

Camerlingo, R., R. Franco, V. Tirino, M. Cantile, M. Rocchi, A. La Rocca, N. Martucci, G. Botti, G. Rocco, and G. Pirozzi. 2011. Establishment and phenotypic characterization of the first human pulmonary blastoma cell line. *Lung Cancer.* 72:23–31. doi:10.1016/j.lungcan.2010.07.009.

Castro-Gamero, A.M., K.S. Borges, R.C. Lira, A.F. Andrade, P.F. Fedatto, G.A.V. Cruzeiro, R.B. Silva, A.M. Fontes, E.T. Valera, M. Bobola, C.A. Scrideli, and L.G. Tone. 2013. Chromosomal heterogeneity and instability characterize pediatric medulloblastoma cell lines and affect neoplastic phenotype. *Cytotechnology.* 65:871–85. doi:10.1007/s10616-012-9529-z.

Chan, M.C.W., C.Y. Cheung, W.H. Chui, S.W. Tsao, J.M. Nicholls, Y.O. Chan, R.W.Y. Chan, H.T. Long, L.L.M. Poon, Y. Guan, and J.S.M. Peiris. 2005. Proinflammatory cytokine responses induced by influenza A (H5N1) viruses in primary human alveolar and bronchial epithelial cells. *Respir. Res.* 6:135. doi:10.1186/1465-9921-6-135.

Chen, J., Z. Chen, T. Narasaraju, N. Jin, and L. Liu. 2004. Isolation of highly pure alveolar epithelial type I and type II cells from rat lungs. *Lab. Investig.* 84:727–35. doi:10.1038/labinvest.3700095.

Chowdhurya, F., W.J. Howata, G.J. Phillips, and P.M. Lackiea. 2010. Interactions between endothelial cells and epithelial cells in a combined cell model of airway mucosa: effects on tight junction permeability. *Exp. Lung Res.* 36:1–11. doi:10.3109/01902140903026582.

Clegg, G.R., C. Tyrrell, S.R. McKechnie, M.F. Beers, D. Harrison, and M.C. McElroy. 2005. Coexpression of RTI40 with alveolar epithelial type II cell proteins in lungs following injury: identification of alveolar intermediate cell types. *Am. J. Physiol. Lung Cell. Mol. Physiol.* 289:L382–90. doi:10.1152/ajplung.00476.2004.

Cordon-Cardo, C., J.P. O'Brien, J. Boccia, D. Casals, J.R. Bertino, and M.R. Melamed. 1990. Expression of the multidrug resistance gene product (P-glycoprotein) in human normal and tumor tissues. *J. Histochem. Cytochem.* 38:1277–87. doi:10.1177/38.9.1974900.

Cotta, C. V., V. Leventaki, V. Atsaves, A. Vidaki, E. Schlette, D. Jones, L.J. Medeiros, and G.Z. Rassidakis. 2008. The helix-loop-helix protein Id2 is expressed differentially and induced by myc in T-cell lymphomas. *Cancer.* 112:552–561. doi:10.1002/cncr.23196.

Crandall, E.D., and M.A. Matthay. 2001. Alveolar epithelial transport. Basic science to clinical medicine. *Am. J. Respir. Crit. Care Med.* 163:1021–1029. doi:10.1164/ajrccm.163.4.2006116.

Crapo, J.D., B.E. Barry, P. Gehr, M. Bachofen, and E.R. Weibel. 1982. Cell number and cell characteristics of the normal human lung. *Am. Rev. Respir. Dis.* 126:332–7.

Cryan, S.-A., N. Sivadas, and L. Garcia-Contreras. 2007. In vivo animal models for drug delivery across the lung mucosal barrier. *Adv. Drug Deliv. Rev.* 59:1133–51. doi:10.1016/j.addr.2007.08.023.

Damia, G., and M. D'Incalci. 2010. Genetic Instability Influences Drug Response in Cancer Cells. *Curr. Drug Targets.* 11:1317–1324(8).

Daum, N., A. Kuehn, S. Hein, U.F. Schaefer, H. Huwer, and C. Lehr. 2012. Isolation, Cultivation, and Application of Human Alveolar Epithelial Cells. *Methods Mol. Biol.* 806:31–42. doi:10.1007/978-1-61779-367-7.

Daum, N., A. Neumeyer, B. Wahl, M. Bur, and C.-M. Lehr. 2009. In vitro systems for studying epithelial transport of macromolecules. *Methods Mol. Biol.* 480:151–64. doi:10.1007/978-1-59745-429-2_11.

Demaio, L., W. Tseng, Z. Balverde, J.R. Alvarez, K.-J. Kim, D.G. Kelley, R.M. Senior, E.D. Crandall, and Z. Borok. 2009. Characterization of mouse alveolar epithelial cell monolayers. *Am. J. Physiol. Lung Cell. Mol. Physiol.* 296:L1051–8. doi:10.1152/ajplung.00021.2009.

Demling, N., C. Ehrhardt, M. Kasper, M. Laue, L. Knels, and E.P. Rieber. 2006. Promotion of cell adherence and spreading: a novel function of RAGE, the highly selective differentiation marker of human alveolar epithelial type I cells. *Cell Tissue Res.* 323:475–88. doi:10.1007/s00441-005-0069-0.

DiVito, K.A., C.M. Simbulan-Rosenthal, Y.-S. Chen, V.A. Trabosh, and D.S. Rosenthal. 2013. Id2, Id3 and Id4 overcome a Smad7-mediated block in tumorigenesis, generating TGF- -independent melanoma. *Carcinogenesis.* 35:951–958. doi:10.1093/carcin/bgt479.

Dobbs, L.G. 1990. Isolation and culture of alveolar type II cells. *Am. J. Physiol.* 258:L134–47.

Dobbs, L.G., M.D. Johnson, J. Vanderbilt, and R. Gonzalez. 2010. Cellular Physiology Biochemistry and Biochemistr y The Great Big Alveolar TI Cell: Evolving Concepts and Paradigms. *Cell. Physiol. Biochem.* 94611:55–62.

doi:DOI:10.1159/000272063.

Dull, T., R. Zufferey, M. Kelly, R.J. Mandel, M. Nguyen, D. Trono, and L. Naldini. 1998. A third-generation lentivirus vector with a conditional packaging system. *J. Virol.* 72:8463–71.

Eglen, R., and T. Reisine. 2011. Primary Cells and Stem Cells in Drug Discovery: Emerging Tools for High-Throughput Screening. *Assay Drug Dev. Technol.* 9:108–124. doi:10.1089/adt.2010.0305.

Ehrhardt, C. 2003. Characterisation of epithelial cell culture models of the lung for in vitro studies of pulmonary drug delivery. Saarland University.

Ehrhardt, C., J. Fiegel, S. Fuchs, R. Abu-Dahab, U.F. Schaefer, J. Hanes, and C.-M. Lehr. 2002. Drug Absorption by the Respiratory Mucosa: Cell Culture Models and Particulate Drug Carriers. *J. Aerosol Med.* 15:131–139. doi:doi:10.1089/089426802320282257.

Ehrhardt, C., C. Kneuer, M. Laue, U.F. Schaefer, K. Kim, and C. Lehr. 2003. 16HBE14o-human bronchial epithelial cell layers express P-glycoprotein, lung resistance-related protein, and caveolin-1. *Pharm. Res.* 20:545–551. doi:10.1023/A:1023230328687.

Ejendal, K.F.K., and C.A. Hrycyna. 2002. Multidrug resistance and cancer: the role of the human ABC transporter ABCG2. *Curr. Protein Pept. Sci.* 3:503–11. doi:10.2174/1389203023380521.

Elbert, K.J., U.F. Schäfer, H.-J. Schäfers, K.-J. Kim, V.H.L. Lee, and C.-M. Lehr. 1999. Monolayers of Human Alveolar Epithelial Cells in Primary Culture for Pulmonary Absorption and Transport Studies. *Pharm. Res.* 16:601–608. doi:10.1023/A:1018887501927.

Endter, S., D. Francombe, C. Ehrhardt, and M. Gumbleton. 2009. RT-PCR analysis of ABC, SLC and SLCO drug transporters in human lung epithelial cell models. *J. Pharm. Pharmacol.* 61:583–91. doi:10.1211/jpp/61.05.0006.

Fanning, A.S., B.J. Jameson, A. Lynne, J.M. Anderson, L. a Jesaitis, and J. Melvin. 1998. CELL BIOLOGY AND METABOLISM: The Tight Junction Protein ZO-1 Establishes a Link between the Transmembrane Protein Occludin and the Actin Cytoskeleton. *J. Biol. Chem.* 273:29745–29753. doi:10.1074/jbc.273.45.29745.

Fehrenbach, H. 2001. Alveolar epithelial type II cell: defender of the alveolus revisited. *Respir. Res.*

Florea, B.I., M.L. Cassara, H.E. Junginger, and G. Borchard. 2003. Drug transport and metabolism characteristics of the human airway epithelial cell line Calu-3. *J. Control. Release.* 87:131–138. doi:10.1016/S0168-3659(02)00356-5.

Forbes, B. 2003. The human bronchial epithelial cell line 16HBE14o− as a model

system of the airways for studying drug transport. *Int. J. Pharm.* 257:161–167. doi:10.1016/S0378-5173(03)00129-7.

Forbes, B., and C. Ehrhardt. 2005. Human respiratory epithelial cell culture for drug delivery applications. *Eur. J. Pharm. Biopharm.* 60:193–205. doi:10.1016/j.ejpb.2005.02.010.

Foster, K.A., C.G. Oster, M.M. Mayer, M.L. Avery, and K.L. Audus. 1998. Characterization of the A549 cell line as a type II pulmonary epithelial cell model for drug metabolism. *Exp. Cell Res.* 243:359–366. doi:10.1006/excr.1998.4172.

Fuchs, S., A.J. Hollins, M. Laue, U.F. Schaefer, K. Roemer, M. Gumbleton, and C.-M. Lehr. 2003. Differentiation of human alveolar epithelial cells in primary culture: morphological characterization and synthesis of caveolin-1 and surfactant protein-C. *Cell Tissue Res.* 311:31–45. doi:10.1007/s00441-002-0653-5.

Funaki, H., T. Yamamoto, Y. Koyama, D. Kondo, E. Yaoita, K. Kawasaki, H. Kobayashi, S. Sawaguchi, H. Abe, and I. Kihara. 1998. Localization and expression of AQP5 in cornea, serous salivary glands, and pulmonary epithelial cells. *Am J Physiol Cell Physiol.* 275:C1151–1157.

Furuse, M., T. Hirase, M. Itoh, A. Nagafuchi, S. Yonemura, and S. Tsukita. 1993. Occludin: a novel integral membrane protein localizing at tight junctions. *J. Cell Biol.* 123:1777–88. doi:10.1083/jcb.123.6.1777.

Gazdar, A.F., J.S. Butel, and M. Carbone. 2002. SV40 and human tumours: myth, association or causality? *Nat. Rev. Cancer.* 2:957–64. doi:10.1038/nrc947.

Gil, J. 1983. Number and distribution of plasmalemmal vesicles in the lung. *Fed. Proc.* 42:2414–8.

Godfrey, R.W.A. 1997. Human Airway Epithelial Tight Junctions. *Microsc. Res. Tech.* 499:488–499. doi:10.1002.

Goldbard, S. 2006. Bringing primary cells to mainstream drug development and drug testing. *Curr. Opin. Drug Discov. Devel.* 9:110–6.

Gossen, M., and H. Bujard. 1992. Tight control of gene expression in mammalian cells by tetracycline-responsive promoters. *Proc. Natl. Acad. Sci.* 89:5547–5551. doi:10.1073/pnas.89.12.5547.

Gould, D.J., M. Berenstein, H. Dreja, F. Ledda, O.L. Podhajcer, and Y. Chernajovsky. 2000. A novel doxycycline inducible autoregulatory plasmid which displays "on"/"off" regulation suited to gene therapy applications. *Gene Ther.* 7:2061–70. doi:10.1038/sj.gt.3301354.

Grainger, C.I., L.L. Greenwell, D.J. Lockley, G.P. Martin, and B. Forbes. 2006. Culture of Calu-3 cells at the air interface provides a representative model of the airway epithelial barrier. *Pharm. Res.* 23:1482–1490. doi:10.1007/s11095-006-

0255-0.

Green, K., and J. Jones. 1996. Desmosomes and hemidesmosomes: Structure and function of molecular components. *Faseb J.* 10:871–881.

Groneberg, D.A., M. Nickolaus, J. Springer, F. Döring, H. Daniel, and A. Fischer. 2001. Localization of the peptide transporter PEPT2 in the lung: implications for pulmonary oligopeptide uptake. *Am. J. Pathol.* 158:707–14. doi:10.1016/S0002-9440(10)64013-8.

Gumbleton, M. 2001. Caveolae as potential macromolecule trafficking compartments within alveolar epithelium. *Adv. Drug Deliv. Rev.* 49:281–300. doi:10.1016/S0169-409X(01)00142-9.

Harvey, D.M., and A.J. Levine. 1991. p53 alteration is a common event in the spontaneous immortalization of primary BALB/c murine embryo fibroblasts. *Genes Dev.* 5:2375–2385. doi:10.1101/gad.5.12b.2375.

Van Haute, L., G. De Block, I. Liebaers, K. Sermon, and M. De Rycke. 2009. Generation of lung epithelial-like tissue from human embryonic stem cells. *Respir. Res.* 10:105. doi:10.1186/1465-9921-10-105.

Hein, S., M. Bur, U.F. Schaefer, and C.-M. Lehr. 2011. A new Pharmaceutical Aerosol Deposition Device on Cell Cultures (PADDOCC) to evaluate pulmonary drug absorption for metered dose dry powder formulations. *Eur. J. Pharm. Biopharm.* 77:132–8. doi:10.1016/j.ejpb.2010.10.003.

Hermanns, M.I., S. Fuchs, M. Bock, K. Wenzel, E. Mayer, K. Kehe, F. Bittinger, and C.J. Kirkpatrick. 2009. Primary human coculture model of alveolo-capillary unit to study mechanisms of injury to peripheral lung. *Cell Tissue Res.* 336:91–105. doi:10.1007/s00441-008-0750-1.

Hermanns, M.I., R.E. Unger, K. Kehe, K. Peters, and C.J. Kirkpatrick. 2004. Lung epithelial cell lines in coculture with human pulmonary microvascular endothelial cells: development of an alveolo-capillary barrier in vitro. *Lab. Investig.* 84:736–752. doi:10.1038/labinvest.3700081.

Hittinger, M., J. Juntke, S. Kletting, N. Schneider-Daum, C. de Souza Carvalho, and C.-M. Lehr. 2015. Preclinical safety and efficacy models for pulmonary drug delivery of antimicrobials with focus on in vitro models. *Adv. Drug Deliv. Rev.* 85:44–56. doi:10.1016/j.addr.2014.10.011.

Hochman, J., and P. Artursson. 1994. Mechanisms of absorption enhancement and tight junction regulation. *J. Control. Release.* 29:253–267. doi:10.1016/0168-3659(94)90072-8.

Hoppstädter, J., B. Diesel, R. Zarbock, T. Breinig, D. Monz, M. Koch, A. Meyerhans, L. Gortner, C.-M. Lehr, H. Huwer, and A.K. Kiemer. 2010. Differential cell reaction upon Toll-like receptor 4 and 9 activation in human alveolar and lung

interstitial macrophages. *Respir. Res.* 11:124. doi:10.1186/1465-9921-11-124.

Horálková, L., A. Radziwon, S. Endter, R. Andersen, R. Koslowski, M.W. Radomski, P. Dolezal, and C. Ehrhardt. 2009. Characterisation of the R3/1 cell line as an alveolar epithelial cell model for drug disposition studies. *Eur. J. Pharm. Sci.* 36:444–50. doi:10.1016/j.ejps.2008.11.010.

Horrocks, C., R. Halse, R. Suzuki, and P.R. Shepherd. 2003. Human cell systems for drug discovery. *Curr. Opin. Drug Discov. Devel.* 6:570–5.

Huang, S.X.L., M.N. Islam, J. O'Neill, Z. Hu, Y.-G. Yang, Y.-W. Chen, M. Mumau, M.D. Green, G. Vunjak-Novakovic, J. Bhattacharya, and H.-W. Snoeck. 2014. Efficient generation of lung and airway epithelial cells from human pluripotent stem cells. *Nat. Biotechnol.* 32:84–91. doi:10.1038/nbt.2754.

Iavarone, A., P. Garg, A. Lasorella, J. Hsu, and M.A. Israel. 1993. The helix-loop-helix protein Id2 enhances cell proliferation and binds to the retinoblastoma protein. *Genes Dev.* 8:1270 – 1284. doi:10.1101/gad.8.11.1270.

Jha, K.K., S. Banga, V. Palejwala, and H.L. Ozer. 1998. SV40-Mediated Immortalization. *Exp. Cell Res.* 7:1–7. doi:doi:10.1006/excr.1998.4272.

Jones, T.C., D.L. Dungworth, and U. Mohr eds. . 1996. Respiratory System. Springer Berlin Heidelberg, Berlin, Heidelberg.

Kalina, M., R.J. Mason, and J.M. Shannon. 1992. Surfactant protein C is expressed in alveolar type II cells but not in Clara cells of rat lung. *Am. J. Respir. Cell Mol. Biol.* 6:594–600. doi:10.1165/ajrcmb/6.6.594.

Kannan, S., H. Huang, D. Seeger, A. Audet, Y. Chen, C. Huang, H. Gao, S. Li, and M. Wu. 2009. Alveolar epithelial type II cells activate alveolar macrophages and mitigate P. Aeruginosa infection. *PLoS One.* 4:e4891. doi:10.1371/journal.pone.0004891.

Kasper, J., M.I. Hermanns, C. Bantz, M. Maskos, R. Stauber, C. Pohl, R.E. Unger, and J.C. Kirkpatrick. 2011. Inflammatory and cytotoxic responses of an alveolar-capillary coculture model to silica nanoparticles: comparison with conventional monocultures. *Part. Fibre Toxicol.* 8:6. doi:10.1186/1743-8977-8-6.

Kato, A., and R.P. Schleimer. 2007. Beyond inflammation: airway epithelial cells are at the interface of innate and adaptive immunity. *Curr. Opin. Immunol.* 19:711–20. doi:10.1016/j.coi.2007.08.004.

Kemp, S.J., A.J. Thorley, J. Gorelik, M.J. Seckl, M.J. O'Hare, A. Arcaro, Y. Korchev, P. Goldstraw, and T.D. Tetley. 2008. Immortalization of human alveolar epithelial cells to investigate nanoparticle uptake. *Am. J. Respir. Cell Mol. Biol.* 39:591–597. doi:10.1165/rcmb.2007-0334OC.

Kikkawa, Y., and K. Yoneda. 1974. The type II epithelial cell of the lung. I. Method of isolation. *Lab. Invest.* 30:76–84.

Kim, K., Z. Borok, and E.D. Crandall. 2001. A Useful In Vitro Model for Transport Studies of Alveolar Epithelial Barrier. *In Vitro.* 18:253–255. doi:10.1023/A:1011040824988.

King, L.S., and P. Agre. 1996. Pathophysiology of the aquaporin water channels. *Annu. Rev. Physiol.* 58:619–48. doi:10.1146/annurev.ph.58.030196.003155.

Kiyono, T., S.A. Foster, J.I. Koop, J.K. McDougall, D.A. Galloway, and A.J. Klingelhutz. 1998. Both Rb/p16INK4a inactivation and telomerase activity are required to immortalize human epithelial cells. *Nature.* 396:84–8. doi:10.1038/23962.

Klein, F. 2012. Eine innovative Strategie zur Etablierung physiologisch relevanter Säugerzelllinien. Helmholtz Centre for Infection Research, Braunschweig, Germany.

Klein, S.G., J. Hennen, T. Serchi, B. Blömeke, and A.C. Gutleb. 2011. Potential of coculture in vitro models to study inflammatory and sensitizing effects of particles on the lung. *Toxicol. Vitr.* 25:1516–34. doi:10.1016/j.tiv.2011.09.006.

Kobayashi, S., S. Kondo, and K. Juni. 1995. Permeability of Peptides and Proteins in Human Cultured Alveolar A549 Cell Monolayer. *Pharm. Res.* 12:1115–1119. doi:10.1023/A:1016295406473.

Kuehn, A., S. Kletting, C. de Souza Carvalho-Wodarz, U. Repnik, G. Griffiths, U. Fischer, E. Meese, H. Huwer, D. Wirth, T. May, N. Schneider-Daum, and C.M. Lehr. 2016. Human alveolar epithelial cells expressing tight junctions to model the air-blood barrier. *Altern. to Anim. Exp.* doi:10.14573/altex.1511.

Lasorella, A., A. Iavarone, and M.A. Israel. 1996. Id2 specifically alters regulation of the cell cycle by tumor suppressor proteins. *Mol. Cell. Biol.* 16:2570–8. doi:10.1128/MCB.16.6.2570.

Lehmann, A.D., N. Daum, M. Bur, C.-M. Lehr, P. Gehr, and B.M. Rothen-Rutishauser. 2011. An in vitro triple cell co-culture model with primary cells mimicking the human alveolar epithelial barrier. *Eur. J. Pharm. Biopharm.* 77:398–406. doi:10.1016/j.ejpb.2010.10.014.

Light, W., A.E. Vernon, A. Lasorella, A. Iavarone, and C. LaBonne. 2005. Xenopus Id3 is required downstream of Myc for the formation of multipotent neural crest progenitor cells. *Development.* 132:1831–41. doi:10.1242/dev.01734.

Linder, S., and H. Marshall. 1990. Immortalization of primary cells by DNA tumor viruses. *Exp. Cell Res.* 191:1–7. doi:10.1016/0014-4827(90)90027-8.

Lipps, C., T. May, H. Hauser, and D. Wirth. 2013. Eternity and functionality - rational access to physiologically relevant cell lines. *Biol. Chem.* 394:1637–48. doi:10.1515/hsz-2013-0158.

Livak, K.J., and T.D. Schmittgen. 2001. Analysis of relative gene expression data

using real-time quantitative PCR and the 2(-Delta Delta C(T)) Method. *Methods.* 25:402–8. doi:10.1006/meth.2001.1262.

Lu, S., A.W. Gough, W.F. Bobrowski, and B.H. Stewart. 1996. Transport Properties Are Not Altered across Caco-2 Cells with Heightened TEER Despite Underlying Physiological and Ultrastructural Changes. *J. Pharm. Sci.* 85:270–273. doi:10.1021/js950269u.

Lührmann, A., G. Bargsten, M. Kuzu, R. Koslowski, R. Pabst, and T. Tschernig. 2007. The alveolar epithelial type I-like cell line as an adequate model for leukocyte migration studies in vitro. *Exp. Toxicol. Pathol.* 58:277–83. doi:10.1016/j.etp.2006.09.002.

Mason, R.J. 2006. Biology of alveolar type II cells. *Respirology.* 11 Suppl:S12–5. doi:10.1111/j.1440-1843.2006.00800.x.

Matter, K., and M.S. Balda. 1998. Occludin and the Functions of Tight Junctions. *Int. Rev. Cytol.* 186:117–146. doi:10.1016/S0074-7696(08)61052-9.

May, A.M., A.-V. Frey, L. Bogatyreva, M. Benkisser-Petersen, D. Hauschke, M. Lübbert, R. Wäsch, M. Werner, J. Hasskarl, and S. Lassmann. 2013. ID2 and ID3 protein expression mirrors granulopoietic maturation and discriminates between acute leukemia subtypes. *Histochem. Cell Biol.* 141:431–440. doi:10.1007/s00418-013-1169-7.

May, T., M. Butueva, S. Bantner, D. Markusic, J. Seppen, R. a F. MacLeod, H. Weich, H. Hauser, and D. Wirth. 2010. Synthetic gene regulation circuits for control of cell expansion. *Tissue Eng. Part A.* 16:441–452. doi:10.1089/ten.tea.2009.0184.

May, T., H. Hauser, and D. Wirth. 2004. Transcriptional control of SV40 T-antigen expression allows a complete reversion of immortalization. *Nucleic Acids Res.* 32:5529–38. doi:10.1093/nar/gkh887.

May, T., H. Hauser, and D. Wirth. 2007. In Vitro Expansion of Tissue Cells by Conditional Proliferation. 140 2007. H. Hauser and M. Fussenegger, editors. Humana Press. 1-15 pp.

McElroy, M.C., and M. Kasper. 2004. The use of alveolar epithelial type I cell-selective markers to investigate lung injury and repair. *Eur. Respir. J.* 24:664–73. doi:10.1183/09031936.04.00096003.

Mennecier, G., L.N. Torres, B. Cogliati, D.S. Sanches, C.M. Mori, A.O. Latorre, L.M. Chaible, I.I. Mackowiak, M.K. Nagamine, T.C. Da Silva, H. Fukumasu, and M.L.Z. Dagli. 2014. Chronic exposure of lung alveolar epithelial type II cells to tobacco-specific carcinogen NNK results in malignant transformation: a new in vitro lung carcinogenesis model. *Mol. Carcinog.* 53:392–402. doi:10.1002/mc.21987.

Moschini, E., M. Gualtieri, M. Colombo, U. Fascio, M. Camatini, and P. Mantecca. 2013. The modality of cell-particle interactions drives the toxicity of nanosized CuO and TiO_2 in human alveolar epithelial cells. *Toxicol. Lett.* 222:102–16. doi:10.1016/j.toxlet.2013.07.019.

Murphy, S.A., D. Dinsdale, P. Hoet, B. Nemery, and R.J. Richards. 1999. A comparative study of the isolation of type II epithelial cells from rat, hamster, pig and human lung tissue. *Methods Cell Sci.* 21:31–8.

Nagy, Z., U.G. Goehlert, L.S. Wolfe, and I. Hüttner. 1985. Ca2+ depletion-induced disconnection of tight junctions in isolated rat brain microvessels. *Acta Neuropathol.* 68:48–52. doi:10.1007/BF00688955.

Neuhaus, W., F. Samwer, S. Kunzmann, R.M. Muellenbach, M. Wirth, C.P. Speer, N. Roewer, and C.Y. Förster. 2012. Lung endothelial cells strengthen, but brain endothelial cells weaken barrier properties of a human alveolar epithelium cell culture model. *Differentiation.* 84:294–304. doi:10.1016/j.diff.2012.08.006.

Nevins, J.R. 1994. Cell cycle targets of the DNA tumor viruses. *Curr. Opin. Genet. Dev.* 4:130–134. doi:10.1016/0959-437X(94)90101-5.

Newman, G.R., L. Campbell, C. von Ruhland, B. Jasani, and M. Gumbleton. 1999. Caveolin and its cellular and subcellular immunolocalisation in lung alveolar epithelium: implications for alveolar epithelial type I cell function. *Cell Tissue Res.* 295:111–20. doi:10.1007/s004410051217.

Nielsen, S., L.S. King, B.M. Christensen, and P. Agre. 1997. Aquaporins in complex tissues. II. Subcellular distribution in respiratory and glandular tissues of rat. *Am. J. Physiol. Lung Cell. Mol. Physiol.* 273:C1549–1561.

Ochs, M., and E.R. Weibel. 2008. Functional Design of the Human Lung for Gas Exchange. *In* McGray-HillMedica.

Papritz, M., C. Pohl, C. Wübbeke, M. Moisch, H. Hofmann, M.I. Hermanns, H. Thiermann, C.J. Kirkpatrick, and K. Kehe. 2010. Side-specific effects by cadmium exposure: apical and basolateral treatment in a coculture model of the blood-air barrier. *Toxicol. Appl. Pharmacol.* 245:361–9. doi:10.1016/j.taap.2010.04.002.

Patton, J.S., and P.R. Byron. 2007. Inhaling medicines: delivering drugs to the body through the lungs. *Nat. Rev. Drug Discov.* 6:67–74. doi:10.1038/nrd2153.

Patton, J.S., C.S. Fishburn, and J.G. Weers. 2004. The lungs as a portal of entry for systemic drug delivery. *Proc. Am. Thorac. Soc.* 1:338–44. doi:10.1513/pats.200409-049TA.

Phelps, D.S., and J. Floros. 1991. Localization of pulmonary surfactant proteins using immunohistochemistry and tissue in situ hybridization. *Exp. Lung Res.* 17:985–995. doi:10.3109/01902149109064330.

Pohl, C., M.I. Hermanns, C. Uboldi, M. Bock, S. Fuchs, J. Dei-Anang, E. Mayer, K. Kehe, W. Kummer, and C.J. Kirkpatrick. 2009. Barrier functions and paracellular integrity in human cell culture models of the proximal respiratory unit. *Eur. J. Pharm. Biopharm.* 72:339–349. doi:10.1016/j.ejpb.2008.07.012.

Ray, R.B., K. Meyer, and R. Ray. 2000. Hepatitis C Virus Core Protein Promotes Immortalization of Primary Human Hepatocytes. *Virology.* 271:197–204. doi:10.1006/viro.2000.0295.

Roggen, E.L., N.K. Soni, and G.R. Verheyen. 2006. Respiratory immunotoxicity: an in vitro assessment. *Toxicol. Vitr.* 20:1249–64. doi:10.1016/j.tiv.2006.03.009.

Rosenberger, C.M., R.L. Podyminogin, P.S. Askovich, G. Navarro, S.M. Kaiser, C.J. Sanders, J.L. McClaren, V.C. Tam, P. Dash, J.G. Noonan, B.G. Jones, S.L. Surman, J.J. Peschon, A.H. Diercks, J.L. Hurwitz, P.C. Doherty, P.G. Thomas, and A. Aderem. 2014. Characterization of innate responses to influenza virus infection in a novel lung type I epithelial cell model. *J. Gen. Virol.* 95:350–362. doi:10.1099/vir.0.058438-0.

Rothberg, K.G., J.E. Heuser, W.C. Donzell, Y.-S. Ying, J.R. Glenney, and R.G.W. Anderson. 1992. Caveolin, a protein component of caveolae membrane coats. *Cell.* 68:673–682. doi:10.1016/0092-8674(92)90143-Z.

Rothen-Rutishauser, B., F. Blank, C. Mühlfeld, and P. Gehr. 2008. In vitro models of the human epithelial airway barrier to study the toxic potential of particulate matter. *Expert Opin. Drug Metab. Toxicol.* 4:1075–89. doi:10.1517/17425255.4.8.1075.

Salomon, J.J., and C. Ehrhardt. 2012. Organic cation transporters in the blood–air barrier: expression and implications for pulmonary drug delivery. *Ther. Deliv.* 3:735–747. doi:10.4155/tde.12.51.

Sato, K., H. Tomioka, T. Shimizu, T. Gonda, F. Ota, and C. Sano. 2002. Type II alveolar cells play roles in macrophage-mediated host innate resistance to pulmonary mycobacterial infections by producing proinflammatory cytokines. *J. Infect. Dis.* 185:1139–47. doi:10.1086/340040.

Schmitz, G., and G. Müller. 1991. Structure and function of lamellar bodies, lipid-protein complexes involved in storage and secretion of cellular lipids. *J. Lipid Res.* 32:1539–70.

Schwerk, J., M. Köster, H. Hauser, M. Rohde, M. Fulde, M.W. Hornef, and T. May. 2013. Generation of Mouse Small Intestinal Epithelial Cell Lines That Allow the Analysis of Specific Innate Immune Functions. *PLoS One.* 8:1–12. doi:10.1371/journal.pone.0072700.

Shapiro, D.L., L.L. Nardone, S.A. Rooney, E.K. Motoyama, and J.L. Munoz. 1978. Phospholipid biosynthesis and secretion by a cell line (A549) which resembles

type II alveolar epithelial cells. *Biochim. Biophys. Acta.* 530:197–207. doi:10.1016/0005-2760(78)90005-X.

Shay, J.W., W.E. Wright, and H. Werbin. 1991. Defining the molecular mechanisms of human cell immortalization. *Biochim. Biophys. Acta.* 1072:1–7. doi:10.1016/0304-419X(91)90003-4.

de Souza Carvalho, C., B. Kasmapour, A. Gronow, M. Rohde, M. Rabinovitch, and M.G. Gutierrez. 2011. Internalization, phagolysosomal biogenesis and killing of mycobacteria in enucleated epithelial cells. *Cell. Microbiol.* 13:1234–49. doi:10.1111/j.1462-5822.2011.01615.x.

Srinivasan, B., A.R. Kolli, M.B. Esch, H.E. Abaci, M.L. Shuler, and J.J. Hickman. 2015. TEER measurement techniques for in vitro barrier model systems. *J. Lab. Autom.* 20:107–26. doi:10.1177/2211068214561025.

Stacey, G., and C. MacDonald. 2001. Immortalisation of primary cells. *Cell Biol. Toxicol.* 17:231–46.

Stampfer, M.R., and P. Yaswen. 2003. Human epithelial cell immortalization as a step in carcinogenesis. *Cancer Lett.* 194:199–208. doi:10.1016/S0304-3835(02)00707-3.

Steimer, A., H. Franke, E. Haltner-Ukomado, M. Laue, C. Ehrhardt, and C.M. Lehr. 2007. Monolayers of porcine alveolar epithelial cells in primary culture as an in vitro model for drug absorption studies. *Eur. J. Pharm. Biopharm.* 66:372–382. doi:10.1016/j.ejpb.2006.11.006.

Steimer, A., M. Laue, H. Franke, E. Haltner-Ukomado, and C.-M. Lehr. 2006. Porcine alveolar epithelial cells in primary culture: morphological, bioelectrical and immunocytochemical characterization. *Pharm. Res.* 23:2078–93. doi:10.1007/s11095-006-9057-7.

Strauss, M., and B.E. Griffin. 1990. Cellular immortalization--an essential step or merely a risk factor in DNA virus-induced transformation? *Cancer Cells.* 2:360–5.

Susewind, J., C. de Souza Carvalho-Wodarz, U. Repnik, E.-M. Collnot, N. Schneider-Daum, G.W. Griffiths, and C.-M. Lehr. 2015. A 3D co-culture of three human cell lines to model the inflamed intestinal mucosa for safety testing of nanomaterials. *Nanotoxicology.* 1–10. doi:10.3109/17435390.2015.1008065.

Tiscornia, G., O. Singer, and I.M. Verma. 2006. Production and purification of lentiviral vectors. *Nat. Protoc.* 1:241–5. doi:10.1038/nprot.2006.37.

Todaro, G.J. 1963. Quantitative studies of the growth of mouse embry cells in culture and their development into established lines. *J. Cell Biol.* 17:299–313. doi:10.1083/jcb.17.2.299.

Torvinen, M., H. Campwala, and I. Kilty. 2007. The role of IFN-gamma in regulation

of IFN-gamma-inducible protein 10 (IP-10) expression in lung epithelial cell and peripheral blood mononuclear cell co-cultures. *Respir. Res.* 8:80. doi:10.1186/1465-9921-8-80.

Trzpis, M., P.M.J. McLaughlin, L.M.F.H. de Leij, and M.C. Harmsen. 2007. Epithelial cell adhesion molecule: more than a carcinoma marker and adhesion molecule. *Am. J. Pathol.* 171:386–95. doi:10.2353/ajpath.2007.070152.

Vass-Marengo, J., A. Ratiarson, C. Asselin, and M. Bastin. 1986. Ability of a T-antigen transport-defective mutant of simian virus 40 to immortalize primary cells and to complement polyomavirus middle T in tumorigenesis. *J. Virol.* 59:655–9.

Vermeer, P.D., J. Denker, M. Estin, T.O. Moninger, S. Keshavjee, P. Karp, J.N. Kline, and J. Zabner. 2009. MMP9 modulates tight junction integrity and cell viability in human airway epithelia. *Am. J. Physiol. Lung Cell. Mol. Physiol.* 296:L751–62. doi:10.1152/ajplung.90578.2008.

Wang, Z., and Q. Zhang. 2004. Transport of proteins and peptides across human cultured alveolar A549 cell monolayer. *Int. J. Pharm.* 269:451–456. doi:10.1016/j.ijpharm.2003.09.033.

Weibel, E.R. 1974. A Note on Differentiation and Divisibility of Alveolar Epithelial Cells. *CHEST J.* 65:19S. doi:10.1378/chest.65.4_Supplement.19S.

Wemhöner, A., P. Jennings, T. Haller, M. Rüdiger, and G. Simbruner. 2011. Effect of exogenous surfactants on viability and DNA synthesis in A549, immortalized mouse type II and isolated rat alveolar type II cells. *BMC Pulm. Med.* 11:11. doi:10.1186/1471-2466-11-11.

Williams, M.C. 2003. A LVEOLAR T YPE I C ELLS : Molecular Phenotype and Development. *Rev. Lit. Arts Am.* doi:10.1146/annurev.physiol.65.092101.142446.

Yamanaka, S., K. Takahashi, K. Tanabe, M. Ohnuki, M. Narita, T. Ichisaka, and K. Tomoda. 2007. Induction of pluripotent stem cells from adult human fibroblasts by defined factors. *Cell.* 131:861–72. doi:10.1016/j.cell.2007.11.019.

LIST OF FIGURES

LIST OF TABLES

ABBREVIATIONS

ABB   Air-Blood Barrier

ALI   Air-Liquid Interface

AT I   Alveolar Type I

AT II   Alveolar Type II

AQP-5   Aquaporin 5

CAV-1   Caveolin 1

DAPI   4',6-Diamidino-2-phenylindole

EDTA   Ethylenediaminetetraacetic acid

EpCAM   Epithelial Cell Adhesion Molecule

FluNa   Sodium Fluorescein

GAPDH   Glyceraldehyde-3-phosphate dehydrogenase

hAELVi   human Alveolar Epithelial cells Lentivirus immortalized

hAEpC   primary human Alveolar Epithelial Cells

hTERT   human Telomerase Reverse Transcriptase

LLC   Liquid-Liquid Culture

Occ   Occludin

SP-C   Surfactant Protein C

SV40 LTAg   Simian Virus 40 Large T Antigen

TEER   Transepithelial Electrical Resistance

ZO-1   Zona Occludens 1

LIST OF PUBLICATIONS

<u>Research papers:</u>

Kuehn, A., S. Kletting, C. de Souza Carvalho-Wodarz, U. Repnik, G. Griffiths, U. Fischer, E. Meese, H. Huwer, D. Wirth, T. May, N. Schneider-Daum, and C.M. Lehr. 2016. Human alveolar epithelial cells expressing tight junctions to model the air-blood barrier. *Altern. to Anim. Exp.* doi:10.14573/altex.1511

<u>Book chapters:</u>

Daum, N., **A. Kuehn**, S. Hein, U.F. Schaefer, H. Huwer, and C. Lehr. 2012. "Isolation, cultivation, and application of human alveolar epithelial cells". Human Cell Culture Protocols. *Methods.* 806:31–42. doi:10.1007/978-1-61779-367-7.

<u>Posters:</u>

Kühn A., Wirth D., May T., Huwer H., Lehr C.-M., Daum N. „Immortalization of primary human alveolar epithelial cells: Development of a new in vitro model of the air-blood barrier" 19th Congress of international society of aerosols in medicine, April 2013, Chapel Hill, USA

Kühn A., Wirth D., May T., Huwer H., Lehr C.-M., Daum N. „Immortalization of primary human alveolar epithelial cells: Development of a new in vitro model of the air-blood barrier" 17th European Congress on Alternatives to Animal Testing, 14th Annual Congress of EUSAAT, September 2012, Linz, Austria

Kühn, A., May,T., Wirth, D., Daum, N., Lehr, C.-M. „Characterization and immortalization of human alveolar cells to develop a new in vitro model of the air-blood-barrier" 9th International Conference and Workshop on Biological Barriers, March 2012, Saarbücken, Germany

Daum N., **Kühn A.**, Huwer H., Lehr C.-M. „Morphological comparison of primary human alveolar cells under different culture conditions: submerged vs. air-liquid interface" 18th Congress of international society of aerosols in medicine, June 2011, Rotterdam, Netherlands

<u>Oral Presentations:</u>

Kühn A., Wirth D., May T., Huwer H., Lehr C.-M., Daum N. „Immortalization of primary human alveolar epithelial cells: Development of a new in vitro model of the

air-blood barrier" 19th Congress of international society of aerosols in medicine, April 2013, Chapel Hill, USA

Kühn A., Wirth D., May T., Huwer H., Lehr C.-M., Daum N. „Immortalization of primary human alveolar epithelial cells: Development of a new in vitro model of the air-blood barrier" 17th European Congress on Alternatives to Animal Testing, 14th Annual Congress of EUSAAT, September 2012, Linz, Austria

Curriculum Vitae

Personal information	
Name:	Anna Michele Kühn
Date of birth:	10.01.1983
Address:	Calle 23 # 77 07
	Belén San Bernardo, Medellín, Antioquia
	Colombia
Place of birth:	Neunkirchen/Saar

08.2013 – today	Emigration to Colombia, Motherhood

PhD thesis	
05.2010 – 07.2013	Helmholtz-Institute for Pharmaceutical Research Saarland, Saarbrücken, Germany
	Title: "Immortalization of primary human alveolar epithelial cells: A new *in vitro* model of the air-blood barrier forming functional tight junctions"

Diploma thesis	
02.2009 – 12.2009	Department of Molecular Plant Biology and Botany, Saarland University, Germany
	Title: "Regulation von bHLH-Transkriptionsfaktoren der Eisenhomöostase in Pflanzen mittels transgener Reporterkonstrukte"

Undergraduate study	
2002 – 2009	Study of Human and Molecular Biology, Saarland University, Germany

School	
1993 – 2002	Secondary high school "Gymnasium am Krebsberg", Neunkirchen/Saar
1989 – 1993	Basic primary school "Grundschule Scheib", Neunkirchen/Saar

Ein besonders großer Dank geht an Chrissi (beste Mitbewohnerin der Welt und fröhlichste Person die ich kenne) Dominik (Office-Bestie und Seelentröster), JD (tú sabes porque), Sandra (Zimmerverleiherin und „Braunschweigerin"), Emad, Nico, Jenny, Birgit, Clemens, Julia und Simon, dafür dass sie nicht nur Arbeitskollegen waren, sondern Freunde sind. Die Schumannstraße 9 war mir ein wundervolles Zuhause.

Ich danke von ganzem Herzen meinem Mann Augusto, den ich ohne diese Doktorarbeit nicht kennengelernt hätte, für die Unterstützung während der letzten Jahre und in Zukunft. Ich danke ihm für das größte Abenteuer meines Lebens und für die größte Liebe meines Lebens – unseren Sohn José.

(De todo corazón quiero decirle gracias a mi esposo Augusto, a quien no habría conocido sin esta tesis, por su apoyo durante los últimos años así como en el futuro. Le agradezco la aventura más grande de mi vida y el amor más grande de mi vida: nuestro hijo José.)

Ich bedanke mich bei meiner ganzen Familie, auf die ich immer bauen kann und die immer an mich glaubt.

Ich danke meiner Schwester Linda, dafür dass sie seit (fast) 30 Jahren die beste kleine Schwester ist, die man sich wünschen kann, egal wie viele tausend Kilometer uns trennen.

Der allergrößte Dank kommt zum Schluss und geht an meine Mutter Barbara, ohne deren Hilfe ich diese Arbeit nicht hätte abschließen können. Sie ist immer für mich da wenn ich sie brauche und sie ist mein großes Vorbild. Nur ihr verdanke ich wer und wo ich heute bin.

"You can't possibly be a scientist if you mind people thinking that you're a fool."

-Douglas Adams, *So Long And Thanks For All The Fish*